

**Effect of torsional and cyclic fatigue preloading on the fracture resistance  
of HyFlex EDM NiTi files**

by

Charles Tra

DMD, Université de Montréal, 2002

A THESIS SUBMITTED IN PARTIAL FULFILLMENT OF  
THE REQUIREMENTS FOR THE DEGREE OF

MASTER OF SCIENCE

in

THE FACULTY OF GRADUATE AND POSTDOCTORAL STUDIES  
(Craniofacial Science)

THE UNIVERSITY OF BRITISH COLUMBIA

(Vancouver)

June 2017

© Charles Tra, 2017

## Abstract

**Objective:** Endodontic nickel-titanium (NiTi) files are submitted to a combination of cyclic fatigue and torsional stresses when used in a root canal, which could lead to their fracture. The purpose of this study was to evaluate the effect of various degrees of cyclic fatigue preloading on the torsional failure and of torsional preloading on the cyclic fatigue life of heat-treated HyFlex EDM NiTi files (Coltene/Whaledent, Altstätten, Switzerland).

**Methods:** The mean number of cycles until failure ( $N_f$ ) of HyFlex EDM and HyFlex CM NiTi (Coltene/Whaledent) files (size #40, taper 0.04 for both files) was examined in a 5mm radius and 60° single curve. Torque and distortion angle at the failure of new instruments and instruments stressed to 50% and 75% of the  $N_f$  were measured according to ISO 3630-1. Other new files were preloaded at 5%, 15%, 25% and 50% of the mean distortion angle before the fatigue test. After torsional preloading, the  $N_f$  was examined. The fracture surface of each fragment was examined with a scanning electron microscope.

**Results:** The fatigue resistance of HyFlex EDM files was higher than that of HyFlex CM files ( $P < .05$ ). The torque and distortion angle at fracture of new HyFlex EDM files were similar to those of new HyFlex CM files. For both instruments, there was a significant effect because of the torsional preloads. Over 15% torsional preloading lowered the  $N_f$  of HyFlex EDM files ( $P < .05$ ), while a moderate amount of 50% torsional preloading significantly lowered the  $N_f$  of HyFlex CM files ( $P < .05$ ). In the fatigue pre-stressed groups, there was no negative effect of the HyFlex EDM group even with 75% preloading on the torque and distortion angle. The fractographic patterns corresponded to the pattern defined by the last stage test.

**Conclusions:** A low amount of torsional preloading reduced the fatigue resistance of HyFlex EDM files. The torsional resistance of HyFlex EDM files was less affected by previous load of cyclic fatigue even after extensive pre-cycling.

## **Lay Summary**

New endodontic rotary files are available to the clinician. In-vitro tests are necessary to understand their physical properties to be able to assess their clinical performance and safety. Fracture of rotary files could occur during their use. This study investigated the fracture resistance of the HyFlex EDM file, a novel file system, and considered the effects of the different stresses generated during the instrumentation phase of an endodontic treatment. The findings contribute to a better understanding of the file's fracture behavior and guide the clinician in its safer use.

## **Preface**

This thesis is the original work and was written by the candidate, Charles Tra as part of the Master of Science in Craniofacial Science program at the University of British Columbia in Vancouver.

The project was conducted under the supervision of the principal supervisor, Dr. Ya Shen, the co-supervisor, Dr. Markus Haapasalo, and the committee member, Dr. Jeffrey Coil. In addition to the author and research supervisors, Dr. Ahmed Hieawy (part of the torsional testing), Dr. Xiangya Huang (part of the torsional testing with cyclic fatigue preloading), and Dr. Zhejun Wang (SEM images and statistical analysis) contributed to this research. The relative contribution is as follows: Charles Tra (60%), Dr. Ya Shen (20%), Dr. Markus Haapasalo (10%) and research team (10%).

Figures and photos were provided by Dr. Ya Shen, Dr. Markus Haapasalo, Charles Tra, and from various articles in the literature. Copyrights were obtained for the use of figures from the literature.

A manuscript based on this research was submitted to the Journal of Endodontics and is waiting for acceptance.

# Table of Contents

|  |             |
|--|-------------|
| <b>Abstract.....</b>   | <b>ii</b>   |
| <b>Lay Summary .....</b>   | <b>iv</b>   |
| <b>Preface.....</b>  | <b>v</b>    |
| <b>Table of Contents .....</b>   | <b>vi</b>   |
| <b>List of Tables .....</b>  | <b>ix</b>   |
| <b>List of Figures.....</b>  | <b>x</b>    |
| <b>List of Symbol.....</b>   | <b>xii</b>  |
| <b>List of Abbreviations .....</b>   | <b>xiii</b> |
| <b>Acknowledgements .....</b>  | <b>xiv</b>  |
| <b>Dedication .....</b>  | <b>xvi</b>  |
| <b>Chapter 1: Introduction .....</b>   | <b>1</b>    |
| 1.1 Endodontic infection and its treatment.....  | 1           |
| 1.2 Endodontic instrumentation .....   | 2           |
| 1.3 NiTi instruments.....  | 2           |
| 1.4 Martensite and austenite metal structures .....  | 4           |
| 1.5 Torsional and cyclic fatigue fracture.....   | 6           |
| 1.6 Resistance to cyclic fatigue, torsion and combination of cyclic fatigue and torsional stresses ..... | 8           |
| 1.7 Prevalence and incidence of file fracture .....  | 12          |
| 1.8 Impact of file fracture on the prognosis of endodontic treatment .....                               | 13          |
| 1.9 Factors influencing file fracture .....  | 14          |

|   |   |           |
|---|---|-----------|
| 1.10  | Canal curvature.....  | 15        |
| 1.11  | Generations of rotary NiTi files.....   | 18        |
| 1.12  | HyFlex EDM .....  | 20        |
| 1.13  | Aims.....   | 25        |
| 1.14  | Hypothesis .....  | 26        |
| <b>Chapter 2: Materials and Methods .....</b> |   | <b>27</b> |
| 2.1   | Baseline scores for cyclic fatigue resistance and torsional resistance .....        | 27        |
| 2.2   | Cyclic fatigue preloading .....   | 30        |
| 2.3   | Torsional preloading .....  | 30        |
| 2.4   | Scanning electron microscopy .....  | 31        |
| 2.5   | Statistical analysis .....  | 31        |
| <b>Chapter 3: Results.....</b>                |   | <b>32</b> |
| 3.1   | Baseline scores for cyclic fatigue and torsional resistance .....                   | 32        |
| 3.2   | Effect of cyclic fatigue preloading on torsional resistance .....                   | 33        |
| 3.3   | Effect of torsional preloading on cyclic fatigue resistance .....                   | 35        |
| 3.4   | SEM images .....  | 36        |
| <b>Chapter 4: Discussion.....</b>             |   | <b>48</b> |
| 4.1   | HyFlex EDM.....   | 48        |
| 4.2   | Fatigue life of HyFlex EDM .....  | 49        |
| 4.3   | Torsional resistance of HyFlex EDM files.....                                       | 50        |
| 4.4   | Effect of cyclic fatigue preloading on the torsional resistance of HyFlex EDM ..... | 51        |
| 4.5   | Effect of torsional preloading on the fatigue life of HyFlex EDM .....              | 52        |
| <b>Chapter 5: Conclusion.....</b>             |   | <b>54</b> |

**Bibliography .....55**



## List of Tables

|  |    |
|--|----|
| Table 1 - Baseline scores for $N_f$ (rotations $\pm$ SD) for HyFlex EDM (EDM) and HyFlex CM (CM) files.....                        | 32 |
| Table 2 - Baseline scores for the distortion angle $\Theta$ (degrees $\pm$ SD) at fracture for HyFlex EDM and HyFlex CM files..... | 32 |
| Table 3 - Baseline scores for the torque (g.cm $\pm$ SD) at fracture for HyFlex EDM and HyFlex CM files. ....                      | 33 |
| Table 4 - Angle (degrees $\pm$ SD) at torsional fracture after different levels of fatigue pre-stress.<br>.....                    | 33 |
| Table 5 -Torque (g.cm $\pm$ SD) at torsional fracture after different levels of fatigue pre-stress.<br>.....                       | 34 |
| Table 6 - $N_f$ (rotations $\pm$ SD) after preloading with different levels of torsional pre-stress. .                             | 36 |

## List of Figures

|   |    |
|---|----|
| Figure 1 - Schneider method.....  | 16 |
| Figure 2 - Angle and radius of curvature.....   | 18 |
| Figure 3 - Basic components of EDM. ....  | 21 |
| Figure 4 - Sparking occurs at closest points between the electrode and workpiece. ....  | 22 |
| Figure 5 - Next spark occurs at closest points between electrode and workpiece.....   | 23 |
| Figure 6 - Crater-like surface of HyFlex EDM.....   | 24 |
| Figure 7 - HyFlex EDM #40/.04 (top) and HyFlex CM #40/.04 (bottom).....   | 27 |
| Figure 8 - Stainless steel artificial canal with curvature of 60° and a radius of 5mm. ....   | 28 |
| Figure 9 - Cyclic fatigue test experimental design. ....  | 29 |
| Figure 10 - Equipment to measure torsional resistance.....  | 29 |
| Figure 11 - Three mm of the instrument tip is firmly secured (arrow).....   | 30 |
| Figure 12 - Distortion angle (degrees) at torsional fracture after different levels of cyclic fatigue preloading. ....  | 34 |
| Figure 13 - Torque (g·cm) at torsional fracture after different levels of cyclic fatigue preloading. ....   | 35 |
| Figure 14 - $N_f$ (rotations) after preloading with different levels of torsional angle. ....   | 36 |
| Figure 15 - Longitudinal view of a fractured HyFlex EDM by cyclic fatigue stress only. ....   | 37 |
| Figure 16 - Longitudinal view of a fractured HyFlex CM by cyclic fatigue stress only.....   | 38 |
| Figure 17 - Fractured surface of HyFlex EDM by cyclic fatigue stress only showing multiple crack origins (asterisk), an area showing microscopic fatigue striations (white outline) and a dimple rupture (red outline)..... | 38 |

|  |    |
|--|----|
| Figure 18 - Fractured surface of HyFlex CM by cyclic fatigue stress only.....  | 39 |
| Figure 19 - Unwinding of a HyFlex EDM file after pure torsional fracture.....  | 40 |
| Figure 20 - Fractured surface of HyFlex EDM file after pure torsional fracture .....   | 40 |
| Figure 21 - A close-up image of circular abrasion marks from picture in Figure 20. ....  | 41 |
| Figure 22 - A close-up image of skewed dimples at the center area from Figure 20. ....   | 41 |
| Figure 23 - Unwinding of a HyFlex CM file after pure torsional fracture. ....  | 42 |
| Figure 24 - Fractured surface of HyFlex CM file after pure torsional fracture. ....  | 42 |
| Figure 25 - A close-up image of circular abrasion marks from picture in Figure 24. ....  | 43 |
| Figure 26 - A close-up image of skewed dimples at the center area in Figure 24.....  | 43 |
| Figure 27 - Microcracks visible (arrows) on the surface of a HyFlex EDM file fractured due<br>to cyclic fatigue after 15% torsional preloading. .... | 45 |
| Figure 28 - Fractured surface of a HyFlex EDM file after 15% torsional preloading and<br>failure by cyclic fatigue. ....                             | 45 |
| Figure 29 - Microcracks visible (arrows) on the surface of a HyFlex CM file fractured due to<br>cyclic fatigue after 15% torsional preloading. ....  | 46 |
| Figure 30 - Fractured surface of a HyFlex CM file after 15% torsional preloading and failure<br>by cyclic fatigue.....                               | 46 |
| Figure 31 - Fractured surface of a HyFlex EDM file after 75% fatigue preloading and failure<br>by shear stress. ....                                 | 47 |
| Figure 32 - Fractured surface of a HyFlex CM file after 50% fatigue preloading and failure<br>by shear stress. ....                                  | 47 |

## List of Symbol

$\Theta$ : distortion angle

## **List of Abbreviations**

DSC: differential scanning calorimetry

EDM: electrical discharge machining

$N_f$ : total number of rotations at failure

NiTi: nickel-titanium

SEM: scanning electron microscope

SD: standard deviation

SS: stainless steel

TTR: transformation temperature range

## **Acknowledgements**

First, to Dr. Jeffrey Coil, I cannot thank you enough for giving me this opportunity to study at UBC in the graduate Endodontic program. In simple words, you totally changed my life! I was enjoying being a general dentist but always felt that something was missing. As I studied in the program, I discovered what was missing. The academic and clinical program that you have built was the key for me to reach the superior level in endodontics, and will serve as a strong foundation for my future career in the specialty. Every day, you acted more than just being the program director. I truly feel all the care you have for the well-being of your residents.

To Dr. Ya Shen, thank you so much for being my principal supervisor. I was aware of your reputation as a researcher. However, in all honesty, I was not conscious of your world leading position in this field. With all our discussions related to the research and my readings of all the articles authored or co-authored by you, I now understand how vast your knowledge and understanding on endodontic files study are. My ignorance of your status was probably due to the fact that every time I met you, you were such a kind and approachable person. You were always available to answer my questions and always wanted to help. I learnt so much from you during this research and you made the whole journey so pleasant!

To Dr. Markus Haapasalo, with your immense knowledge and sincere pleasure to teach, you have greatly helped me to complete this research. At first, I was intimidated and was not so sure on how to approach you because of your international reputation. However, once I started talking to you, I realized that you are such a humble person who loves to teach others.

You never hid the fact that, sometimes, there are still unanswered questions in the endodontic specialty. I really admire that quality of yours. Your teachings were so valuable and it was a great pleasure to listen to them.

Also, I want to thank and mention the contribution of my co-residents, Dr. Zhejun Wang, Dr. Ahmed Hieawy and Dr. Xiangya Huang. They generously took their time and helped me with their expertise in different aspects of my research.

Importantly, to my parents, I am who I am today because of you. Without your life-changing decision to move to Canada at a young age and your hard work to provide your children with a life where we did not have to worry about anything, I would not be where I am today. Your values and principles in life are the fundamentals of my person. With all my heart, thank you, Maman, and Papa!

Finally, to the most important person in my life, my wife, I know it was a huge shock when I decided to flip our lives upside down when we moved to Vancouver three years ago. You never once complained and kept supporting our journey. You took care of every detail of our lives, giving me the time I needed to devote myself to this research. This accomplishment is as much yours as it is mine. Thank you, Christine, for all the support and all your sacrifices! We have a lot to look forward to!

## **Dedication**

Dear Dr. Paul Hébert,

I want to dedicate this research to you. Doing so, I want to profoundly thank you for being my mentor throughout all the years. Your passion for dentistry and the role model that you are to my eyes have inspired me to become the best dentist I can be. Your teachings and life lessons are guiding my every decision to always do the “right thing” in my professional and personal life. I feel deeply privileged for all the time you gave me and will always cherish all our lunches that we shared in restaurants near your office. Finally, I can tell you, with confidence, that now, I found my place in the world!!!

And thank you again...

Sincerely,

Charles



# **Chapter 1: Introduction**

## **1.1 Endodontic infection and its treatment**

The goal of endodontic treatment is to cure and prevent pulpal disease and disease of the periapical tissues (Ørstavik and Pitt Ford, 1998). Bacteria are the predominant etiological factor responsible for these conditions (Kakehashi et al, 1965). Bacteria invade the pulp canal system through caries, fractures, cracks, and several other pathways and cause areas of inflammation. If the source of bacteria is not removed, the pulp will eventually become necrotic. These inflamed and necrotic areas coalesce and slowly progress in the direction of the apical region of the tooth. Soon, bacterial by-products and in some cases bacteria also reach the periapical tissues through the apical foramen causing an inflammatory reaction and bone resorption: this is the formation of apical periodontitis (Siqueira and Lopes, 2011).

At this stage, the root canal system is colonized by bacteria. The host immune system, which is activated and tries to eradicate the harmful invading microbes, cannot effectively reach the bacteria in the root canal because of the lack of blood circulation in the necrotic pulp. Therefore, dental treatment is necessary to eliminate the microbes and thereby eliminate the infection. This can be achieved either by extraction of the tooth or by root canal therapy.

After a proper diagnosis, root canal treatment consists of an initial step of mechanical cleaning and shaping with the aid of irrigation solutions, and a final step of canal obturation with the placement of an adequate coronal restoration. Mechanical instrumentation of the canal system has multiple roles: reduction of bacterial load, removal of debris and organic tissues,

and creation of space for the irrigation solutions (Metzger et al, 2013) and the root filling (Schilder, 1967).

## **1.2 Endodontic instrumentation**

The mechanical instrumentation is done with the aid of multiple endodontic instruments. At present, stainless steel (SS) hand files and rotary nickel-titanium (NiTi) files are commonly used. Traditionally, all endodontic instruments were made of SS. Because of the inherent stiffness of this material, these instruments have been associated with different clinical mishaps, which include ledge or zip formation, perforation of the canal, and separation or fracture of the instrument (Weine et al, 1975). To overcome the clinical problems, NiTi rotary files were introduced in the 1990's to the endodontic world.

## **1.3 NiTi instruments**

NiTi is a metallic alloy composed of nickel and titanium. It was first developed in the early 1960s by W.F. Buehler for the space program at the Naval Ordnance Laboratory (Buehler et al, 1963). The newly developed alloy was called Nitinol, which stands for nickel, titanium and the initial of the Naval Ordnance Laboratory (-nol). It is composed of approximately 56% weight of nickel and 44% weight of titanium which gives an equiatomic ratio of nickel and titanium (Thompson, 2000). NiTi has the unique properties of super-elasticity and shape memory. Shape memory and super-elasticity properties are defined as the ability of an alloy to undergo large deformations and to return to its original shape after heating (shape memory property) or after removal of the stress (super-elasticity property) (DesRoches et al, 2004).

The super-elasticity property of the NiTi caught the attention of Dr. Walia's group (1988). They were the first researchers to investigate the possibility of using NiTi in the fabrication of endodontic instruments. They were thinking that a more flexible instrument made from NiTi would reduce the occurrence of procedural errors related to the inherent stiffness of SS instruments. In 1988, they fabricated endodontic files in size #15 from arch wire blanks of NiTi and investigated their flexibility in bending and their resistance to torsional fracture. These new NiTi files were able to undergo a deformation of more than 90 degrees without having any permanent deformation; this demonstrated the "outstanding elastic flexibility" of the NiTi files. In comparison, permanent deformation of SS files occurred after a 30 degrees bend. Their study also showed that NiTi files had a higher torsional resistance with a mean value of 2½ rotations before torsional fracture compared to SS files which had a mean value of 1¾ rotations. The authors concluded that files made with NiTi showed promise and could be better suited for the treatment of curved canals in endodontics than SS files (Walia et al, 1988).

NiTi files have been shown to be superior to SS files for the instrumentation of root canals. In 1995, Glosso et al (1995) compared Lightspeed files (Lightspeed Technology, San Antonio, TX, USA), a new rotary NiTi file system at that time, with SS hand files and NiTi hand files in preparation of mesial canals of mandibular molars. Instrumentation with the Lightspeed system resulted in a more centered and rounder canal preparation with less canal transportation and less dentin removal than the other two groups (Glosso et al, 1995). Gambill et al (1996) compared the use of NiTi hand files and SS hand files by using computed tomography images of canals before instrumentation and after instrumentation. Two different filling methods were used for the NiTi hand files: quarter turn/pull technique and reaming

technique. The NiTi files used with a reaming technique caused less canal transportation, removed less dentin and produced more centered and rounder preparation (Gambill et al, 1996). Gluskin et al (2001) arrived at similar conclusions, when they compared the canals prepared with the use of hand files and Gates Glidden burs to the ones shaped with NiTi GT rotary files (Dentsply Maillefer, Ballaigues, Switzerland). The results showed less transportation and more conservation of tooth structure with the use of NiTi rotary instruments (Gluskin et al, 2001).

Since then, rotary NiTi files have been widely used for the canal instrumentation part of the endodontic treatment. The focus of the industry has been directed in modifications of the file design, the file cross-section and the metallurgy of the NiTi to improve the efficiency and safety of these files. Passive and active cutting, radial lands, fixed and variable taper, cross-sectional shapes and offset center of rotation are examples of different innovative concepts in the file design. In 2007, the advent of thermomechanical treated NiTi alloy marked an important step in the history of NiTi files. Heat treatment of NiTi improved the physical properties of the NiTi by changing the crystalline form of the alloy. It resulted with files with higher fracture resistance, fewer clinical mishaps and better canal shaping properties (Haapasalo and Shen, 2013).

#### **1.4 Martensite and austenite metal structures**

NiTi can present itself in two different crystallographic forms. The two crystallographic forms of NiTi are the austenite phase and the martensitic phase. An intermediary phase called R-phase also exists. The atomic arrangement differs between the martensitic and austenite phases and confers different physical properties to the alloy (Thompson, 2000).

At high temperatures, NiTi is in the austenite phase. When the NiTi is cooled down below transformation temperature range (TTR), it goes through an atomic re-arrangement, called martensitic transformation. NiTi under a martensitic phase is more ductile (more easily deformed) than NiTi in the austenite phase. Similarly, when NiTi is heated above the TTR, the NiTi reverts to its austenite phase. Under this phase, the atomic bonding is stronger and more directional: the deformed NiTi file returns to its original shape. This describes the phenomenon of shape memory property of NiTi (Thompson, 2000).

The TTR of a NiTi depends on its composition and the ratio of nickel and titanium. It could range between  $-50^{\circ}\text{C}$  to  $+100^{\circ}\text{C}$ . In addition, the TTR can be altered through different manufacturing processes. Modification of the ratio of nickel and titanium, cold working, heat treatments of NiTi are methods to change the TTR (Thompson, 2000).

The application of physical stress on the NiTi induces a similar phase transformation from austenite to martensite. This characteristic is called stress-induced martensitic transformation. As mentioned earlier, the martensitic phase of NiTi is more ductile than the austenite phase. Therefore, the stress-induced martensitic transformation results in a more ductile state of NiTi after the application of physical stress. This explains the super-elasticity property of the NiTi. Once the physical stress is removed, the NiTi returns to its austenite phase, which forces its atomic configuration to return to its original configuration and, thus, the NiTi regains its original shape. This super-elasticity property of the NiTi allows this alloy to sustain more deformation before plastic deformation and fracture compared to other metals (Thompson, 2000).

## **1.5 Torsional and cyclic fatigue fracture**

Even though an endodontic NiTi file is more flexible than a SS file, fracture of a NiTi file is possible during its use, and this could happen without any warning signs (Ankrum et al, 2004). This clinical complication could compromise the prognosis of the tooth (Friedman and Stabholz, 1986). During the instrumentation of the canal, the endodontic file is subjected to torsional and flexural stresses, and torsional fracture or cyclic (flexural) fatigue fracture could occur (Sattapan et al, 2000).

Torsional stress is created when the tip of a rotary file gets locked in the canal and the file continues to rotate. Once the torsional stress exceeds the elastic limit of the metal, torsional (or shear) fracture occurs. This type of fracture is accompanied by longitudinally visible plastic deformation of the file near the fracture line (Sattapan et al, 2000). Other authors (Cheung et al, 2005) found that it could also happen without any signs of plastic deformation.

Cyclic fatigue fracture is associated with the use of rotary files in a curved canal. A rotating file in a curved canal creates repetitive and alternating zones of compression and tension along the file, which cause metal fatigue. The accumulation of metal fatigue leads to the cyclic fatigue fracture of the file. Contrary to torsional fracture, cyclic fatigue fracture happens without any visible defects on the longitudinal surface of the file (Pruett et al, 1997).

Sattapan et al (2000) collected 378 discarded endodontic Quantec files after normal use from a private endodontic clinic. They categorized the type of fracture which occurred: torsional or cyclic fatigue fracture. To do so, they experimentally fractured new files with one specific type of stress (torsional or cyclic fatigue stress) and analyzed the appearance of the files after their fracture. They found that torsional fracture was accompanied by defects consisting of unwinding, reverse winding, reverse winding with tightening of the spirals, or a

combination of these defects. On the other hand, cyclic fatigue fracture was characterized by a sharp break without any visible defects. The authors identified signs of flexural fatigue in 44.3% of the fractured files (Sattapan et al, 2000).

From a large sample size of discarded rotary NiTi instruments (n = 7159), Parashos et al (2004) found an overall defect rate of 17%: 12% of files showed unwinding defects and 5% were fractured. Using the criteria established by Sattapan et al (2000), they established the mode of fracture: torsional fracture was determined by the presence of unwinding and fatigue fracture by its absence. They found more fatigue fractures than torsional fractures: the former happened in 3.5% of the files and the latter had a rate of 1.5% (Parashos et al, 2004).

Peng et al (2005) did a study where they examined longitudinally under scanning electron microscope discarded ProTaper (Dentsply Maillefer) S1 instruments from the endodontic clinic of a dental school over a period of 17 months. They collected 121 S1 instruments and found that 23% were fractured (27/121). According to the criteria set by Sattapan et al (2000), almost all fractured files were cyclic fatigue fractures. Only two files had a torsional fracture. They explained this result with the fact that the S1 instrument has a variable taper which reduces the taper-lock effect, thus reducing the torsional stress on the file (Peng et al, 2005). In the second part of this study published by Cheung et al (2005), the fractographic surface of these same instruments was examined under scanning electron microscope. The fractured surface of a cyclic fatigue fracture would show typical “fatigue striations” or “beach marks” and a dimple area. Conversely, a torsional fracture would be characterized by the absence of these fatigue striations, the presence of concentric rubbing or abrasion marks, and the presence of areas of skewed dimples on the fractured surface. Under these criteria, the type of fracture was re-determined. The number of torsional fractures found increased from two

(Peng et al (2005)) to nine torsional fractures (9/27), thus the remaining eighteen were cyclic fatigue fracture (18/27). Hence, the authors concluded that a longitudinal examination of a fractured file is not suitable to determine the type of fracture and that fractographic examination under scanning electron microscope is necessary (Cheung et al, 2005).

## **1.6 Resistance to cyclic fatigue, torsion and combination of cyclic fatigue and torsional stresses**

Multiple studies have evaluated the fracture resistance to torsional stress and cyclic fatigue stress. However, the clear majority of these studies only evaluated one of these, either the cyclic fatigue or torsional resistance independently. An endodontic file is submitted to concomitant torsional stress and cyclic fatigue stress during the instrumentation phase of an endodontic treatment. Only a few studies tried to elude the effects of the combination of both stresses on the fracture resistance of an endodontic file (Barbosa et al, 2007; Bahia et al, 2008; Kim et al, 2012; Cheung et al, 2013; Campbell et al, 2014; Shen et al, 2015).

### **1.6.1 Cyclic fatigue resistance**

There are many different laboratory tests to study the cyclic fatigue resistance of a file. Each test has its advantages and disadvantages. A test measuring the cyclic fatigue resistance involves rotating a file in a curved shape and measuring the number of rotations of the file until its fracture, also called fatigue life ( $N_f$ ). However, a slight variation in the methodology can greatly influence the results of these tests. Currently, five different designs for measuring cyclic fatigue in the laboratory have been reported: 1) curved metal tube (hypodermic needle); 2)



grooved block-and-rod assembly; 3) rotation against an inclined plane; 4) three-point bend of a rotating instrument; and 5) custom-made artificial canal (Plotino et al, 2009; Shen and Cheung, 2013).

### **1.6.2 Torsional resistance**

The American Dental Association specification #28 and the ISO standard 3630-1 describe the methodology to test the torsional resistance of endodontic files. The instrument tip is clamped usually 3mm at the tip, and either the clamp or the instrument is then rotated to apply torsional stress. At the point where the instrument breaks, the maximum torque (torsional load) and distortion angle are recorded. The distortion angle corresponds to the angle of rotation of the file at the fracture point (Shen & Cheung, 2013).

### **1.6.3 Combination of cyclic fatigue and torsional stresses**

Kim et al (2012) studied the torsional resistance of files which were previously submitted to cyclic fatigue stress (preloading). They established the mean number of rotations until cyclic fatigue fracture of Profile (size #25, taper 0.06; Dentsply Maillefer) and ProTaper (F1: size #20, taper 0.07). They then cyclically preloaded new files at 25%, 50% and 75% of these means, before testing their torsional resistance. The authors found that 75% of cyclic fatigue preloading significantly affected the torsional resistance when compared to the groups with no preloading, or 25% and 50% preloading (Kim et al, 2012).

Campbell et al (2014) performed a similar study where the effect of cyclic fatigue preloading on the torsional resistance of conventional NiTi Typhoon files (Clinician's Choice

Dental Products, New Milford, CT, USA) and controlled memory NiTi Typhoon files (Clinician's Choice Dental Products) was evaluated. Cyclic fatigue preloading did not affect the torsional resistance of files size #25, taper 0.04 for both types of files. However, all the controlled memory Typhoon files size #40, taper 0.04 with cyclic fatigue preloading of 25%, 50%, and 75% showed a significant reduction in the angle of rotation until torsional fracture compared to the non-preloading group (Campbell et al, 2014).

The effect of torsional preloading on the cyclic fatigue resistance of conventional NiTi K3 files (Kerr Dental, Orange, CA, USA) was studied by Barbosa et al (2007) and by Bahia et al (2008). In the former study, unused K3 files were submitted to 90°, 180° and 420° of torsional preloading with the consequence that files preloaded with an increased distortion angle had a lower fatigue life (Barbosa et al, 2007). Bahia et al (2008) preloaded unused K3 files with 20 cycles of torsional stress by applying a distortion angle from 0° to 180° before measuring their fatigue life. Also in this study, preloading of torsional stress reduced the fatigue resistance of the K3 files (Bahia et al, 2008).

Cheung et al (2013) also investigated the effect of torsional preloading on the cyclic fatigue resistance. Profile files (size #25, taper 0.06) and ProTaper files (F1: size #20, taper 0.07) were used for this experiment. The files were divided into four groups: no torsional preloading, and preloading with 25%, 50% and 75% of the mean torsional load (torque) at fracture. Surprisingly, the 50% and 75% preloading groups of the Profile, and all the preloaded groups of ProTaper resulted with a higher resistance to cyclic fatigue fracture. The authors concluded that a torsional preloading may improve the cyclic fatigue resistance of a file (Cheung et al, 2013).

Pedullà et al (2015) looked into the effect of torsional preloading on the fatigue life of conventional NiTi files and heat-treated files, in which one of the files studied was the HyFlex CM file. A preload of 25%, 50% and 75% of the mean torsional load (torque) at fracture was applied, but differently than the previous cited study, the motion was repeated for 20 or 40 times before testing the cyclic fatigue resistance. Except for one group, all torsional preloading (25%, 50%, and 75%) significantly reduced the number of revolutions before fatigue fracture; only the fatigue life of the HyFlex CM group with 25% torsional preloading was not affected by torsional preloading (Pedullà et al, 2015).

Shen et al (2015) evaluated both cyclic fatigue preloading and torsional preloading on the fracture resistance of K3 files and the heat-treated K3XF files (SybronEndo, Orange, CA, US). The results showed that only a low amount of torsional preloading (25% torsional preloading group) was needed to affect the cyclic fatigue resistance of both files negatively. Regarding the cyclic fatigue preloading, only the 75% pre-cycled K3 files group had a reduction in its torsional resistance. Thus, a lower amount of cyclic fatigue preloading (25% and 50%) did not reduce the torsional resistance of the K3 files, and the torsional resistance K3XF was not affected by any previous preloading of cyclic fatigue stress (Shen et al, 2015).

In summary, a high amount of cyclic fatigue preloading (75%) seems to be necessary to have an effect on the torsional resistance of endodontic files (Kim et al, 2012; Campbell et al, 2014; Shen et al, 2015). Even at that level, the torsional resistance of some group of files was not affected by any previous cyclic fatigue preloading (Campbell et al, 2014; Shen et al, 2015). Only the controlled memory NiTi Typhoon files size #40, taper 0.04 group in a study by Campbell et al (2014) demonstrated a reduction of the torsional resistance with a low

amount of cyclic fatigue preloading of 25%. The type of NiTi, either conventional or heat-treated, was not a factor.

The majority of the studies demonstrated that low amount of 25% torsional preloading decreased the cyclic fatigue resistance of conventional and heat-treated endodontic files (Barbosa et al, 2007; Bahia et al, 2008; Pedullà et al, 2015; Shen et al, 2015). In contrast to these findings, one study showed that torsional preloading had a positive effect and improved the cyclic fatigue resistance (Cheung et al, 2013).

### **1.7 Prevalence and incidence of file fracture**

In a retrospective examination of radiographs, Spili et al (2005) found a prevalence of 3.3% of teeth with retained fractured instrument in 8460 cases treated non-surgically in two endodontic practices. The fractured instruments were either a rotary NiTi file, a SS hand file, a paste filler or a lateral spreader. The results showed that 2.8% of teeth (235/8460) had a retained fractured rotary NiTi file. However, when the authors analyzed the data for the period where NiTi rotary files were mainly used, the prevalence of a tooth with a retained separated NiTi rotary file went up to 4.4% (Spili et al, 2005). However, it may be worth noting that at the time of this study, the files were made of conventional NiTi. Heat-treated NiTi files were available to the clinician only after 2007. One can speculate that the incidence of file fracture would be lower if heat-treated NiTi files were used.

Iqbal et al (2006) did a retrospective study on the occurrence of instrument fracture in an endodontic program between the years 2000-2004. The authors examined the records of 4865 endodontically treated teeth. Because the cases were referred to a university endodontic

program, the difficulty level of the treatments was higher than average. The files were discarded after being used in eight teeth or if deformation of a file was visible. The authors found 81 separated instruments: 12 were SS hand instruments and 69 were rotary NiTi instruments. The incidence of instrument fracture was 0.25% for hand files and 1.68% for rotary files. Instrument fracture was seven times higher with NiTi rotary instruments than with SS hand instruments (Iqbal et al, 2006).

### **1.8 Impact of file fracture on the prognosis of endodontic treatment**

Once an endodontic file has fractured in the canal, it is important for the clinician to understand the impact of this mishap on the outcome of the endodontic treatment. Grossman (1969) stated that a retained file fragment reduced the success rate of endodontic treatment (Grossman, 1969). The presence of pre-existing periapical radiolucency is the main factor affecting the prognosis for cases with a fractured instrument (Grossman, 1969; Bergenholtz et al, 1979).

Spili et al (2005) did a retrospective study of all the nonsurgical endodontic treatments of two endodontic offices over a period of 13.5 years. They examined the treatment outcome of teeth with a retained file fragment. The data included 146 teeth with a fractured instrument for which a follow-up of at least one year was available. The authors matched similar cases which had no retained fractured instrument, and compared their outcomes. Overall, the presence of a retained fractured instrument did not have a significant influence on the outcome. Success was defined as radiographic healing or incomplete healing and absence of clinical signs and symptoms. For the cases that did not have a pre-existing periapical radiolucency, there was no significant difference in the success rate: 98.4% for the cases with no retained

fractured instrument, and 96.8% for the cases with a retained fractured instrument. The presence of a pre-existing periapical radiolucency did not change this finding: the success rate for the control group was 92.9%, and the group with a retained fractured instrument had a success rate of 86.7%. The difference was not statistically significant. The study concluded that a fractured instrument does not affect the outcome of endodontic treatment. The authors, however, nuanced their conclusion in their discussion and mentioned that the stage of the instrumentation and the level of cleanliness of the canal when the fracture of the instrument happens could potentially influence the relationship between a fractured instrument and the outcome of the endodontic treatment (Spili et al, 2005).

## **1.9 Factors influencing file fracture**

Parashos et al (2004) studied the factors influencing the occurrence of defects (unwinding or fracture of the rotary files) in the files used by fourteen endodontists. They concluded that it was a multifactorial problem. Rotary file brand, size, taper, cross-sectional shape and instrument design had an influence in the apparition of defects. However, they concluded that the most important factor was the operator (Parashos et al, 2004).

Iqbal et al (2006) discussed other factors influencing the occurrence of file fracture. Files with large size and taper are more prone to cyclic fatigue fracture than small files, but they are more resistant to torsional stress. Also, the risk for file fracture increases as the severity of canal curvature increases. The authors found more file fractures in the apical third where the canal is usually curved and the diameter is smaller. Other factors mentioned in that study were instrumentation technique, preparation of a manual glide path, operator's clinical experience, the number of repeated uses of the instrument, rate of rotation of the files,

knowledge of the canal anatomy and physical properties of the NiTi instrument (Iqbal et al, 2006).

### **1.10 Canal curvature**

In the literature, multiple methods exist to quantify the amount of curvature of a canal: the Schneider method, the Weine method, the long axis method and the Pruett method (Günday et al, 2005). Part of Schneider's study in 1971 looked into the influence of canal curvature on the frequency of obtaining a round canal preparation with hand instruments (Schneider, 1971). He defined the angle of curvature as the angle between a first line traced parallel to the long axis of the canal and a second line traced from the apical foramen to the point where the canal began to leave the long axis of the tooth (Figure 1). He qualified a canal as being straight when the angle was 5 degrees or less, moderate curvature when the angle was 10 to 20 degrees and a severe curvature when the angle was between 25 and 70 degrees.

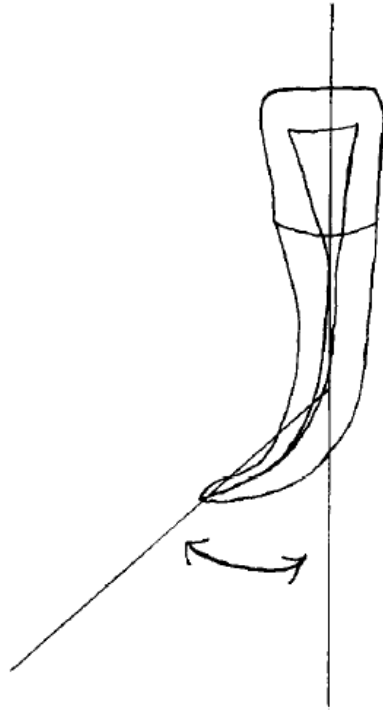


Figure 1 - Schneider method.

(From © Schneider SW (1971). A comparison of canal preparations in straight and curved root canals. *Oral Surg Oral Med Oral Pathol*, 32(2), 271-5. Page 272. By permission from publisher.)

Weine (1982) described another method to calculate the angle of curvature of a root canal. Similar to the Schneider's method, the angle of curvature is measured as the angle formed by the intersection of two lines. A first line is drawn from the canal orifice through the coronal portion of the curvature. While, the second line is drawn from the apical foramen through the apical portion of the curvature. The curvature of the canal is defined by the angle created by these two lines (Weine, 1982).

Hankins et al (1996) proposed a long axis method to describe the angle of curvature of a canal. The authors used a line corresponding to the long axis of the tooth and another line



going through the apical third of the canal. The intersection formed by these two lines defines the angle of curvature (Hankins et al, 1996).

In 1997, Pruett et al added another parameter to describe the angle of curvature. Because two teeth with the same angle of curvature could present totally different canal abruptness, the notion of the radius of curvature was introduced. The Pruett method (Figure 2) uses similar lines as described by the Weine method to quantify the angle of curvature: the first line is parallel the coronal third of the canal and the second line follows the apical portion of the canal. To measure the angle of curvature, the Pruett method takes in consideration the two points on these two lines where the canal curvature begins and ends. More specifically a first point is established where the canal starts to deviate from the line parallel to the coronal portion of the canal, and similarly, a second point is marked where the canal deviates from the line parallel to the apical portion of the canal. A circle tangent to these two points is traced, and the angle of curvature is measured as the angle formed by the arcs of the circle to these two points. The radius of curvature corresponds to the radius of this circle. A canal with a short radius of curvature meant a more abrupt curve and would result in an increased cyclic fatigue stress to the file. In this study, a radius of curvature of two mm was considered as an abrupt curvature; and a canal with a five mm radius of curvature was described as a “sweeping curvature”. This classification of the radius of curvature was independent of the angle of curvature. Thus, the Pruett method addresses a limitation of previous methods (Pruett et al, 1997). Following this study, the radius of curvature was considered as an important variable when testing cyclic fatigue resistance of endodontic files.

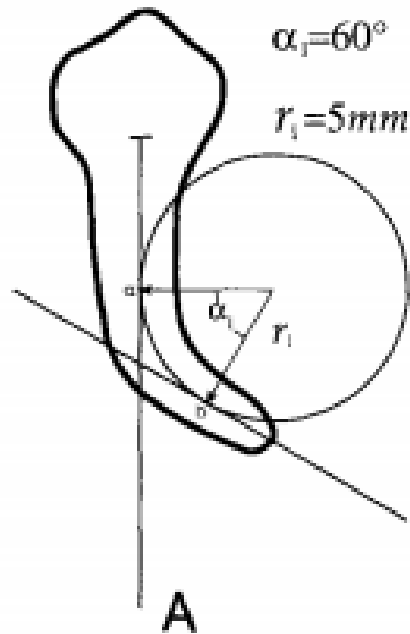


Figure 2 - Angle and radius of curvature.  
 (From © Pruett JP et al (1997). Cyclic fatigue testing of nickel-titanium endodontic instruments. J Endod, 23(2), 77-85. Page 79. By permission from publisher.)

### 1.11 Generations of rotary NiTi files

In a very competitive market, manufacturers have brought multiple new NiTi rotary files to the market with the intention to offer more efficient and safer file systems. Each new generation of files differs from the previous generation with innovative file design and change in the metallurgy of the NiTi. The novelties rely on changes in the cross-section, taper and metallurgy of the files.

The first generation of rotary NiTi files was introduced in 1993. The files were characterized by a passive cutting, a constant taper and radial lands. Profile, Lightspeed and Quantec (Tycon Inc., Chattanooga, TN, USA) are examples of first generation file systems. The transition from passive cutting edges to active cutting edges marks the advent of the second

generation of rotary NiTi files. ProTaper file system is an example of the second generation (Haapasalo and Shen, 2013).

To reduce the incidence of instrument fracture, manufacturers introduced in 2007 heat treatment of the NiTi alloy used in the fabrication of the files. With the purpose to alter the metallurgy of NiTi, heat treatment changes the transition temperature from the martensitic phase to austenite phase of the alloy. Heat-treated NiTi characterized the third generation of files. They exhibit higher fatigue resistance compared to the previous generations. Examples of files of this generation are Hyflex CM, K3XF, Profile GT (Dentsply Maillefer), Vortex (Dentsply Maillefer), Vortex Blue (Dentsply Maillefer), Typhoon, and Twisted Files (Kerr Dental) (Haapasalo and Shen, 2013). CM wire was one of the first examples of improved NiTi alloy by heat treatment. It was introduced in 2010. Files made from CM wire are very flexible and can maintain the deformed shape after being bent. This property is called controlled shape memory (Pirani et al, 2016). HyFlex CM files and Typhoon files are made with CM Wire (Haapasalo and Shen, 2013). The transformation from martensite to austenite for CM wire is completed at around 50 °C. As a result, the file will have a (flexible) martensitic structure when it is used at body temperature in the mouth (Santos et al, 2013). Files made with CM Wire have cyclic fatigue resistance superior to files made with conventional NiTi (Shen et al, 2011).

Fourth generation files appeared on the market in 2011 and are distinguished by the reciprocating movement during their clinical use compared to the traditional continuous rotation of files from previous generations. WaveOne files (Dentsply Maillefer) and Reciproc files (VDW GmbH, Munich, Germany) are examples of reciprocating file systems. Finally, the fifth generation files are designed with an offset center of rotation. It results with a lesser engagement of the file with the dentin, thus reducing the screw effect and the taper lock of a

rotary file. ProTaper Next files (Dentsply Maillefer) and TruShape files (Dentsply Maillefer) are examples of files with an offset center of rotation (Haapasalo and Shen, 2013).

### **1.12 HyFlex EDM**

HyFlex EDM is a novel file system. It is made with the same CM wire NiTi alloy as its predecessor, the HyFlex CM. The main feature with the HyFlex EDM resides in its fabrication method; it is created by an electrical discharge machining method (EDM). It is the only file system manufactured this way (Pirani et al, 2016).

Electrical discharge machining is a manufacturing process where electric current passes through a workpiece and an electrode immersed in a dielectric fluid. It creates carefully controlled sparks which cause the metal surface of the work-piece to melt and evaporate (Figure 3). By creating one spark at a time, it slowly cuts the workpiece in the exact location that is needed. The sparks are created where the electrode and the workpiece are closest (Figure 4 and 5). The metal vaporizes and then is cooled by the dielectric fluid (Jameson, 2001).

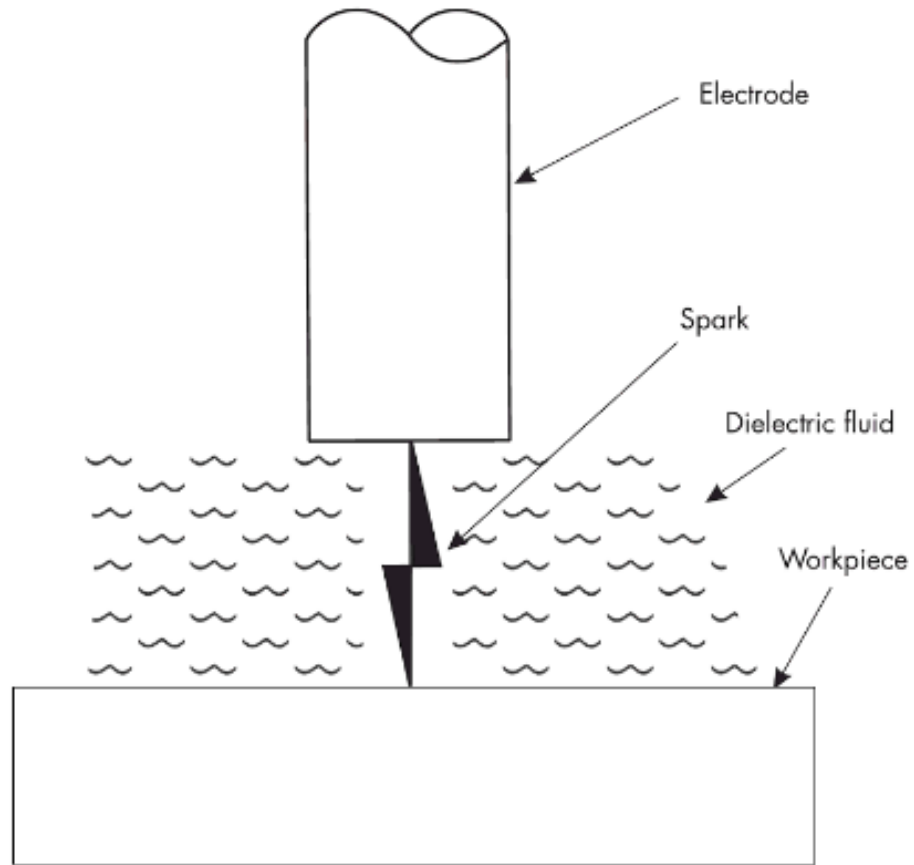


Figure 3 - Basic components of EDM.  
(From © Jameson, EC (2001). Electrical discharge machining. Society of Manufacturing Engineers. Page 2. By permission from publisher.)

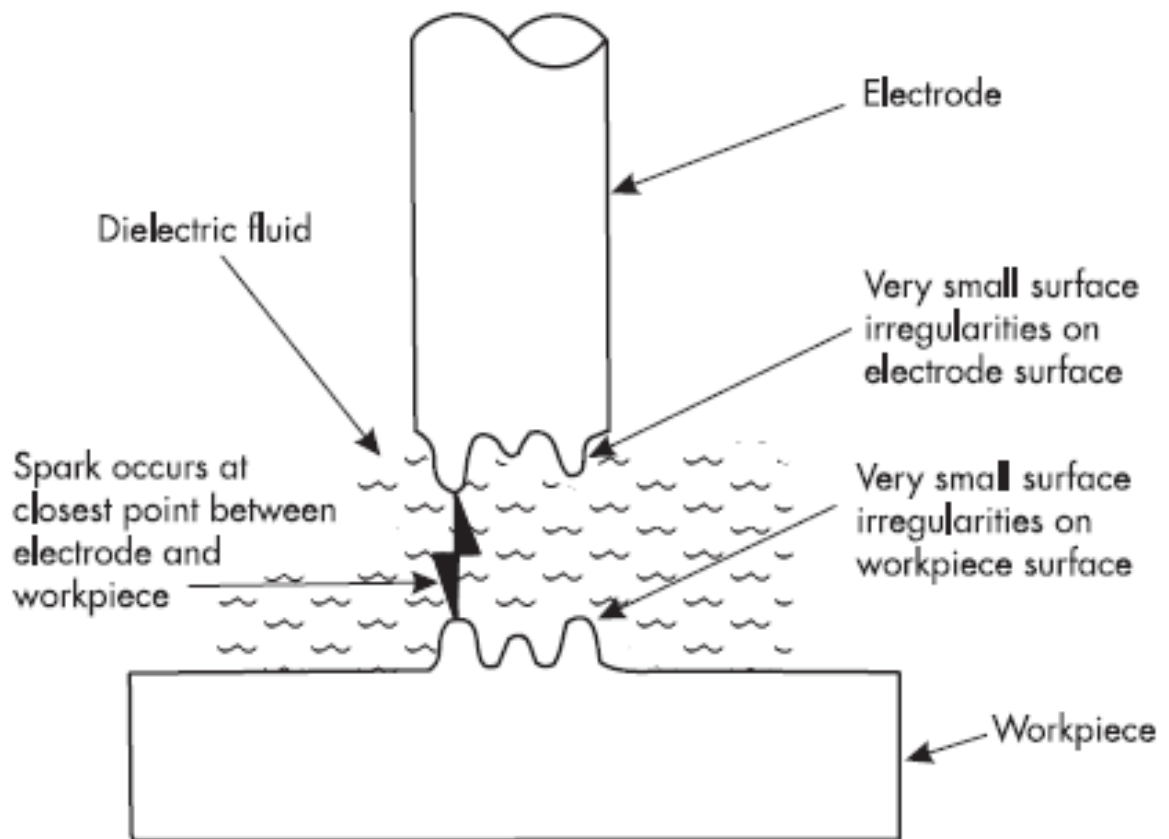


Figure 4 - Sparking occurs at closest points between the electrode and workpiece.  
 (From © Jameson, EC (2001). Electrical discharge machining. Society of Manufacturing Engineers. Page 3. By permission from publisher.)

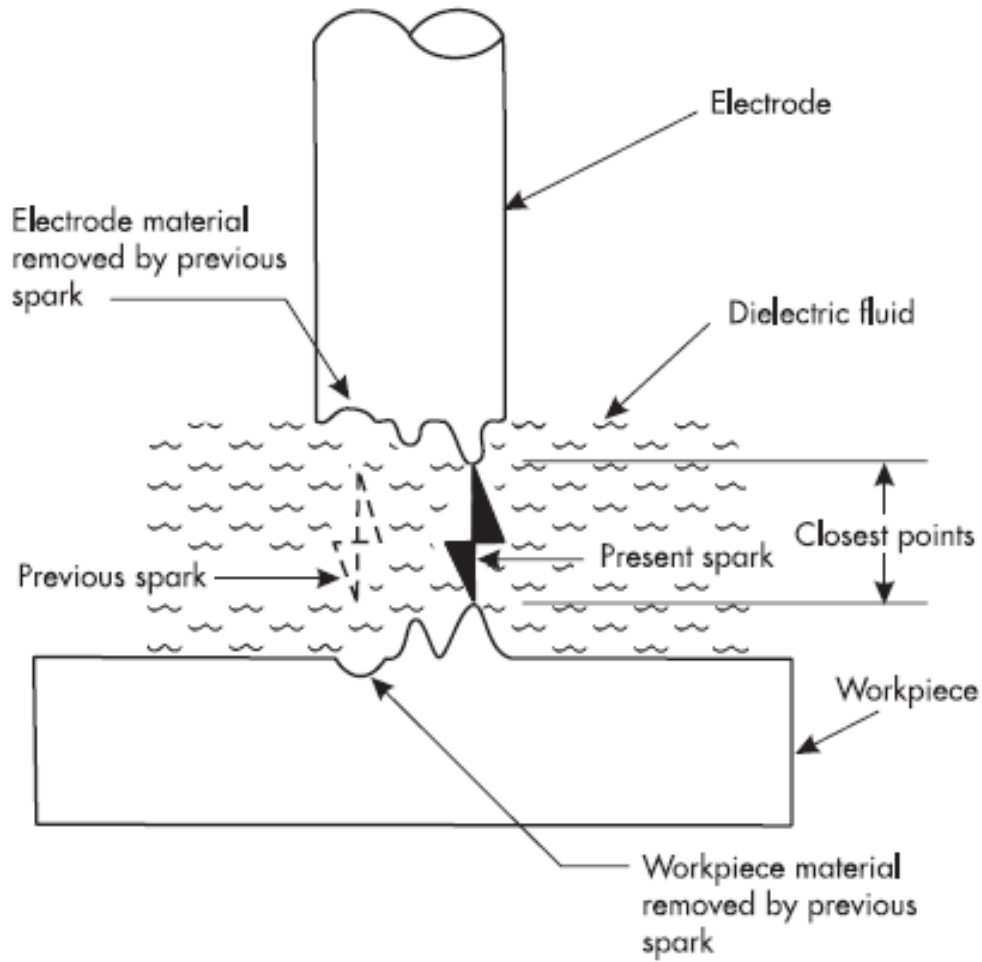


Figure 5 - Next spark occurs at closest points between electrode and workpiece. (From © Jameson, EC (2001). Electrical discharge machining. Society of Manufacturing Engineers. Page 4. By permission from publisher.)

Pirani et al (2016) observed under high magnification unused and used HyFlex EDM files and studied their fracture resistance. Under a scanning electron microscope, the electrical discharge machining process creates a rough surface with multiple craters at the surface of the file (Figure 6). After the files were used in ten canals, the crater-like surface and the integrity of the cutting edges were preserved. Microcracks and spiral distortions were not observed (Pirani et al, 2016).

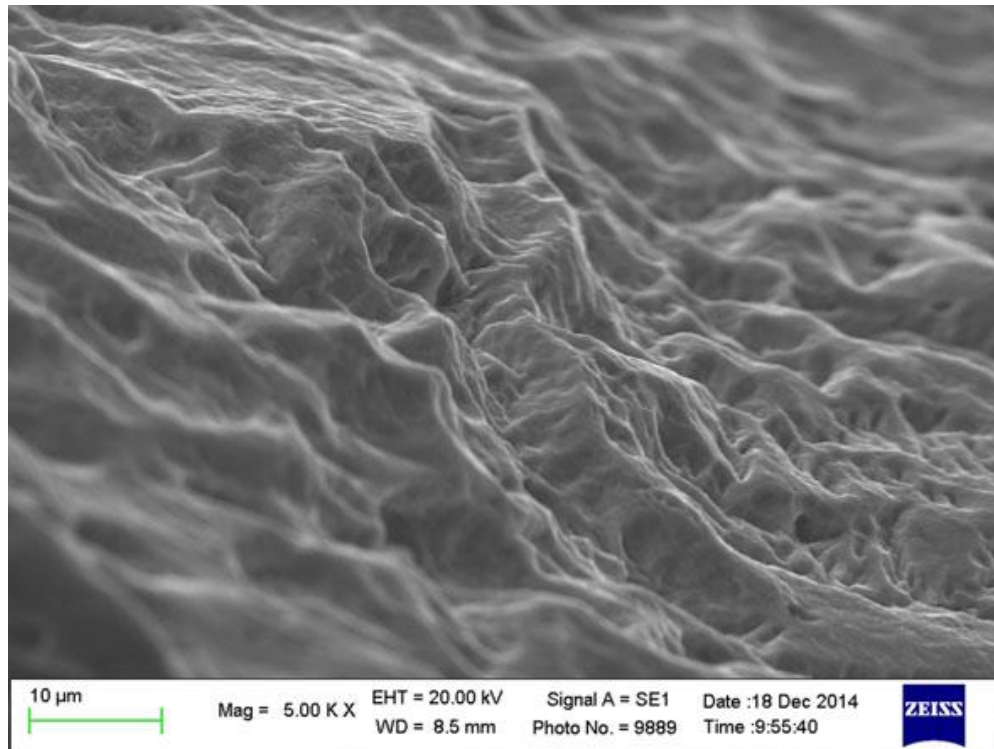


Figure 6 - Crater-like surface of HyFlex EDM.  
(From © Pirani C. et al (2016). HyFlex EDM: superficial features, metallurgical analysis and fatigue resistance of innovative electro discharge machined NiTi rotary instruments. Int Endod J, 49, 483-93. Page 4. By permission from publisher.)

Another advantage with the electrical discharge machining is the ability to manufacture files with complex file design. The fine and precise control of the position of the spark gives more latitude to the manufacturer in giving the file its final shape, compared to the traditional mechanical machining of a file. HyFlex EDM has a progressive cross-sectional shape. At the tip of the instrument, the cross-section of the file is rectangular. Towards the shank of the instrument the cross-section becomes more triangular. According to the manufacturer, this supposedly increases the fracture resistance of the file (HyFlex EDM brochure, Coltene/Whaledent).



The HyFlex EDM files system is marketed as a one file system. The main file is a size #25 with a variable taper: taper 0.08 for the first 5 mm from the tip, and taper 0.04 for the rest of the file. The main file can supposedly treat almost all cases. An orifice opener (size #25, taper 0.12), a glide path file (size #10, taper 0.05) and finishing files (size #40, taper 0.04; size #50, taper 0.03; size #60, taper 0.02) are also available to the clinician. To treat curved canals, the manufacturer recommends employing a HyFlex CM size #20, taper 0.04 before the use of the main HyFlex EDM file (HyFlex EDM brochure, Coltene/Whaledent).

In their study, Pirani et al (2016) tested the cyclic fatigue resistance of HyFlex EDM and found that HyFlex EDM was 683% more resistant to cyclic fatigue fracture than HyFlex CM. They concluded that this improvement in fracture resistance was due to the electrical discharge machining of HyFlex EDM (Pirani et al, 2016). Likewise, Pedullà et al (2016) found that HyFlex EDM (size #25, taper 0.08) had a higher cyclic fatigue resistance and a higher distortion angle at torsional fracture, when it was compared to Reciproc files (size #25, taper 0.08) and WaveOne files (size #25, taper 0.08) (Pedullà et al, 2016).

### **1.13 Aims**

The aim of this study was to evaluate the effect of various degrees of cyclic fatigue preloading on the torsional failure and of torsional preloading on the cyclic fatigue life of heat-treated HyFlex EDM NiTi files.

### **1.14 Hypothesis**

The null hypothesis of the present study was that there is no difference on the torsional failure of HyFlex EDM and HyFlex CM files when the instruments are pre-stressed to 50% and 75% of the  $N_f$ ; and no difference on the cyclic fatigue life of HyFlex EDM and HyFlex CM files when the instruments are preloaded at 5%, 15%, 25% and 50% of the mean distortion angle.

## Chapter 2: Materials and Methods

### 2.1 Baseline scores for cyclic fatigue resistance and torsional resistance

To establish baseline values, unused HyFlex EDM files size #40, taper 0.04 and unused HyFlex CM files size #40, taper 0.04 (Figure 7) were tested ( $n = 10$  in each group) for their cyclic fatigue resistance and their torsional resistance. The size #40, taper 0.04 was chosen because it is the only combination of size and taper shared by both types of files.



Figure 7 - HyFlex EDM #40/.04 (top) and HyFlex CM #40/.04 (bottom).

The cyclic fatigue tests consisted of placing the rotary files in a custom-made stainless steel artificial canal with a curvature of  $60^\circ$  and a radius of 5 mm (Figure 8). The customization of the artificial insured a tight fit of the tested files. The files were then rotated with the aid of

torque control motor (AEU-20T Endodontic System) at a speed of 500 rpm and a torque of up to 2.5N.cm, as suggested by the manufacturer until fracture (Figure 9). A tempered glass covered the artificial canal and the rotating file. This allowed to keep the file inside the artificial canal and its visualization until fracture. Water was placed in the artificial canal and acted as a lubricant during the testing. The fatigue life, or the total number of rotations to failure ( $N_f$ ), was recorded.

The torsional tests were performed according to ISO 3630-1 using a torsion machine (Figure 10). Three mm of the instrument tip was secured firmly in a specifically designed soft brass holder (Figure 11). The apparatus was composed of a torque sensor (Futek Model TFF 400; Futek, Irvine, CA) and a low-speed rotating motor. The rotation speed was set clockwise to 2 rpm until fracture occurred. The torsional load (torque) and distortion angle were recorded until the instrument fractured.

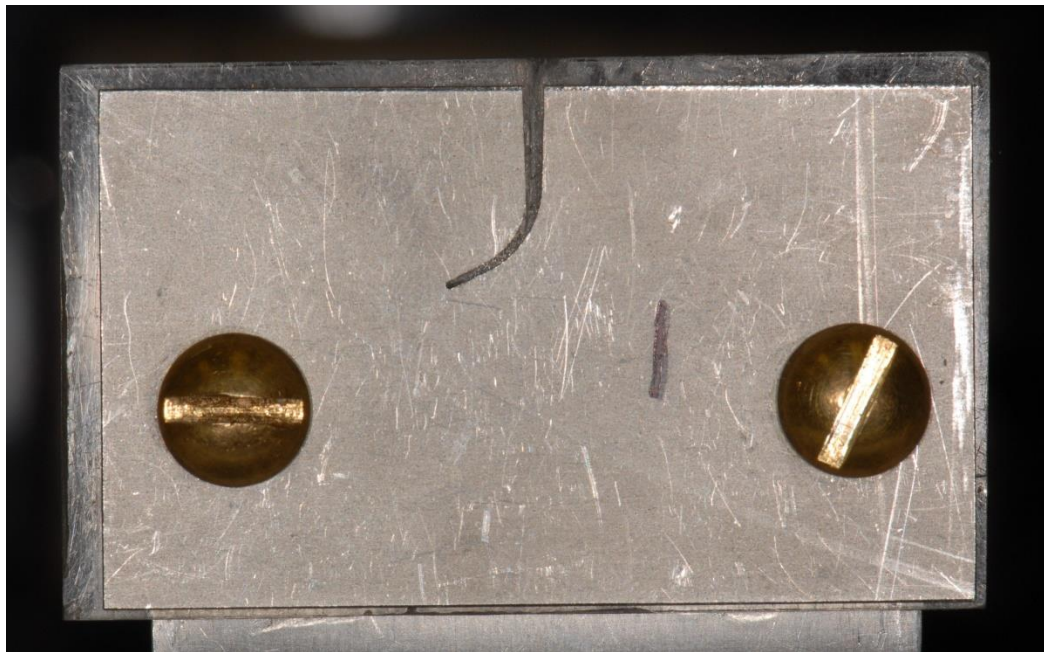


Figure 8 - Stainless steel artificial canal with curvature of  $60^\circ$  and a radius of 5mm.

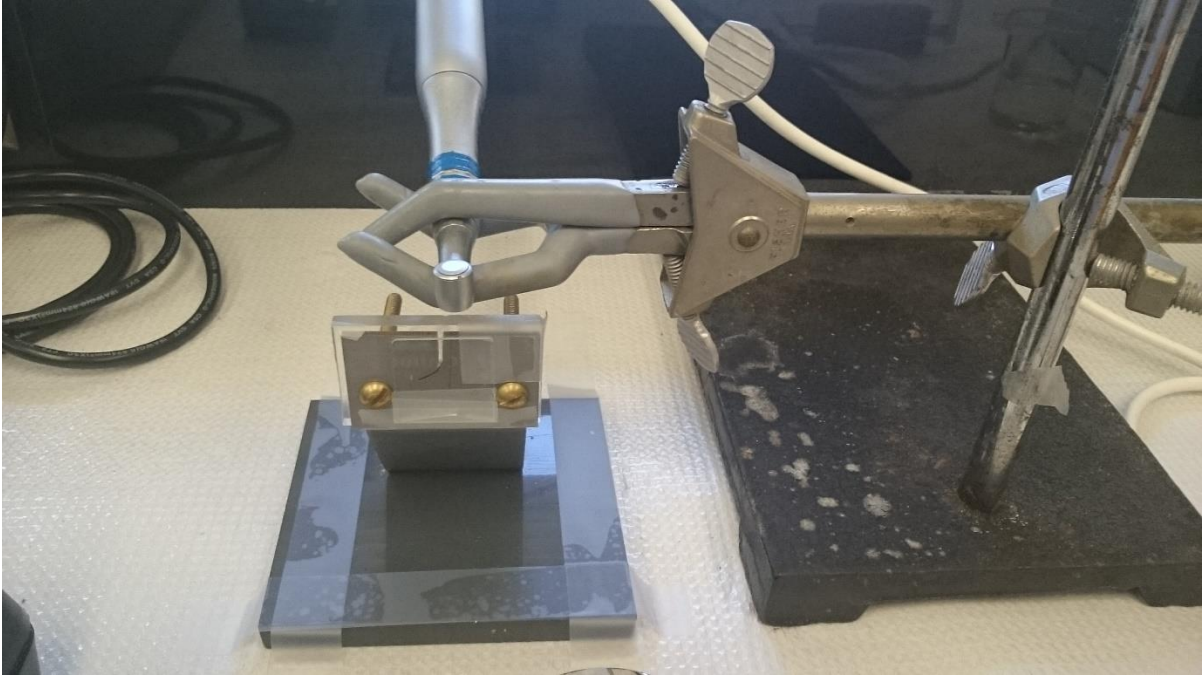


Figure 9 - Cyclic fatigue test experimental design.



Figure 10 - Equipment to measure torsional resistance.



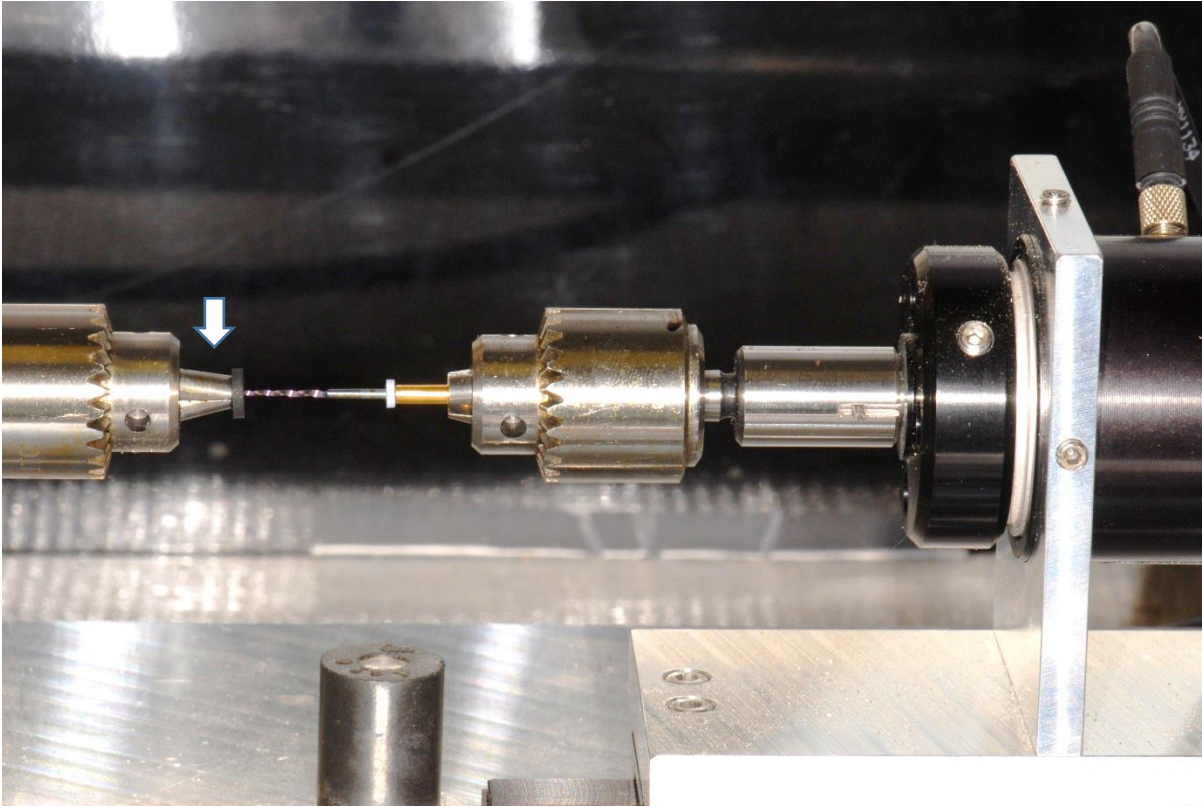


Figure 11 - Three mm of the instrument tip is firmly secured (arrow).

## 2.2 Cyclic fatigue preloading

To evaluate the effects of cyclic fatigue preloading on the torsional resistance, unused HyFlex EDM and HyFlex CM files, both in size #40, taper 0.04, were cycled to 50% and 75% of their respective  $N_f$  in the same artificial canal used for the fatigue test ( $n = 10$  in each group). These fatigue pre-stressed files were then tested for their torsional resistance as described earlier. The torsional load and distortion angle were measured until fracture.

## 2.3 Torsional preloading

Unused HyFlex EDM files and unused HyFlex CM files were torsionally preloaded in the torsion machine by applying 5%, 15%, 25% and 50% of their respective mean distortion

angle at fracture ( $n = 10$  in each group). After torsional preloading, cyclic fatigue resistance was examined in the artificial canal.

#### **2.4 Scanning electron microscopy**

After the fracture of the files, three files in each group were examined longitudinally under a scanning electron microscope (SEM) (Stereoscan 260; Cambridge Instruments, Cambridge, UK). The fractured instrument was placed in an ultrasonic bath with alcohol to remove any debris or residues prior the SEM examination. The fracture surfaces of the fragments were also examined with the SEM at 5 kV and magnifications of x14, x17, x150, x160, x170, x200, x230, x250, x300, x750, and x1000 to establish the mode of fracture.

#### **2.5 Statistical analysis**

Normal distribution of the results was verified with Kolmogorov-Smirnov test. The results were then analyzed using 2-way analysis of variance and post hoc Tukey test (SPSS for Windows 11.0; SPSS, Chicago, IL) when necessary at a significance level of  $P < .05$ .

## Chapter 3: Results

### 3.1 Baseline scores for cyclic fatigue and torsional resistance

In the cyclic fatigue testing, the  $N_f$  of unused HyFlex EDM files was significantly higher than the  $N_f$  of unused HyFlex CM files ( $P < .05$ ) (Table 1). However, the distortion angle (Table 2) and the torsional load (Table 3) at fracture of HyFlex EDM files were not statistically different from those of HyFlex CM files. From these results, the number of rotations corresponding to 50% and 75% of the  $N_f$  were calculated (Table 1). Similarly, 5%, 15%, 25% and 50% of the distortion angle at torsional fracture were established (Table 2). These values were used for the subsequent preloading tests.

Table 1 - Baseline scores for  $N_f$  (rotations  $\pm$  SD) for HyFlex EDM (EDM) and HyFlex CM (CM) files.

|     | $N_f$          | 50% $N_f$ | 75% $N_f$ |
|-----|----------------|-----------|-----------|
| EDM | 2490 $\pm$ 306 | 1245*     | 1868*     |
| CM  | 1029 $\pm$ 158 | 515*      | 772*      |

\* Calculated from the testing results

Table 2 - Baseline scores for the distortion angle  $\Theta$  (degrees  $\pm$  SD) at fracture for HyFlex EDM and HyFlex CM files.

|     | $\Theta$     | 5% $\Theta$ | 15% $\Theta$ | 25% $\Theta$ | 50% $\Theta$ |
|-----|--------------|-------------|--------------|--------------|--------------|
| EDM | 797 $\pm$ 57 | 40*         | 120*         | 199*         | 399*         |
| CM  | 786 $\pm$ 27 | 39*         | 118*         | 197*         | 393*         |

\* Calculated from the testing results



Table 3 - Baseline scores for the torque (g.cm  $\pm$  SD) at fracture for HyFlex EDM and HyFlex CM files.

|     | Torque       |
|-----|--------------|
| EDM | 125 $\pm$ 16 |
| CM  | 116 $\pm$ 9  |

### 3.2 Effect of cyclic fatigue preloading on torsional resistance

In the HyFlex EDM cyclic fatigue preloading groups, there was no difference in distortion angle (Table 4, Figure 12) and torque value (Table 5, Figure 13) between any of the groups (with or without preloading), even with the 75% cyclic fatigue preloading group. The HyFlex CM files had significant lower distortion angles after 50% cyclic fatigue preloading (Table 4, Figure 12) and lower torque value after 75% cyclic fatigue preloading (Table 5, Figure 13), compared to the files without fatigue preloading ( $P < .05$ ).

Table 4 - Angle (degrees  $\pm$  SD) at torsional fracture after different levels of fatigue pre-stress.

|     | 0% N <sub>f</sub> | 50% N <sub>f</sub> | 75% N <sub>f</sub> |
|-----|-------------------|--------------------|--------------------|
| EDM | 797 $\pm$ 57      | 900 $\pm$ 105      | 787 $\pm$ 231      |
| CM  | 786 $\pm$ 27      | 690 $\pm$ 73       | 682 $\pm$ 44       |

Table 5 -Torque (g·cm ± SD) at torsional fracture after different levels of fatigue pre-stress.

|     | 0% N <sub>f</sub> | 50% N <sub>f</sub> | 75% N <sub>f</sub> |
|-----|-------------------|--------------------|--------------------|
| EDM | 125 ± 16          | 141 ± 15           | 134 ± 18           |
| CM  | 116 ± 9           | 120 ± 22           | 98 ± 11            |

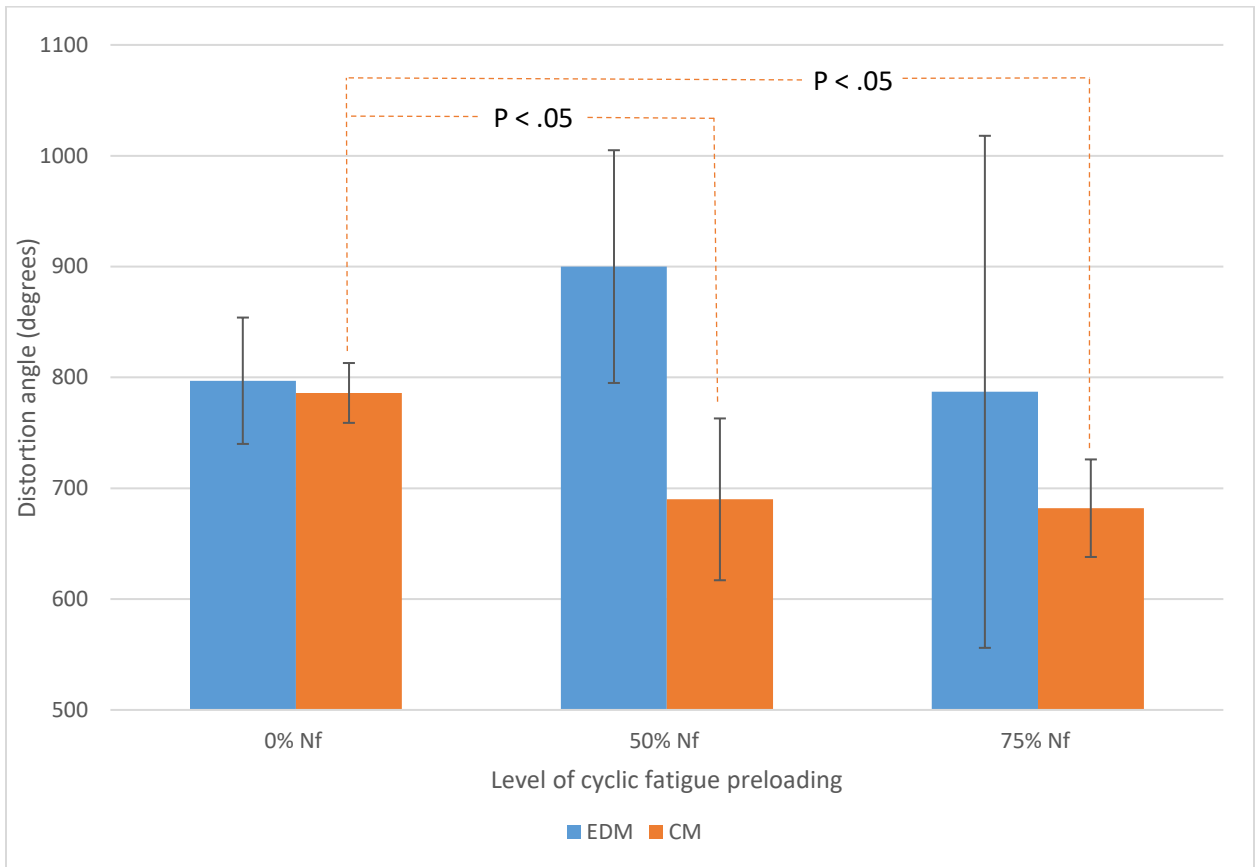


Figure 12 - Distortion angle (degrees) at torsional fracture after different levels of cyclic fatigue preloading.

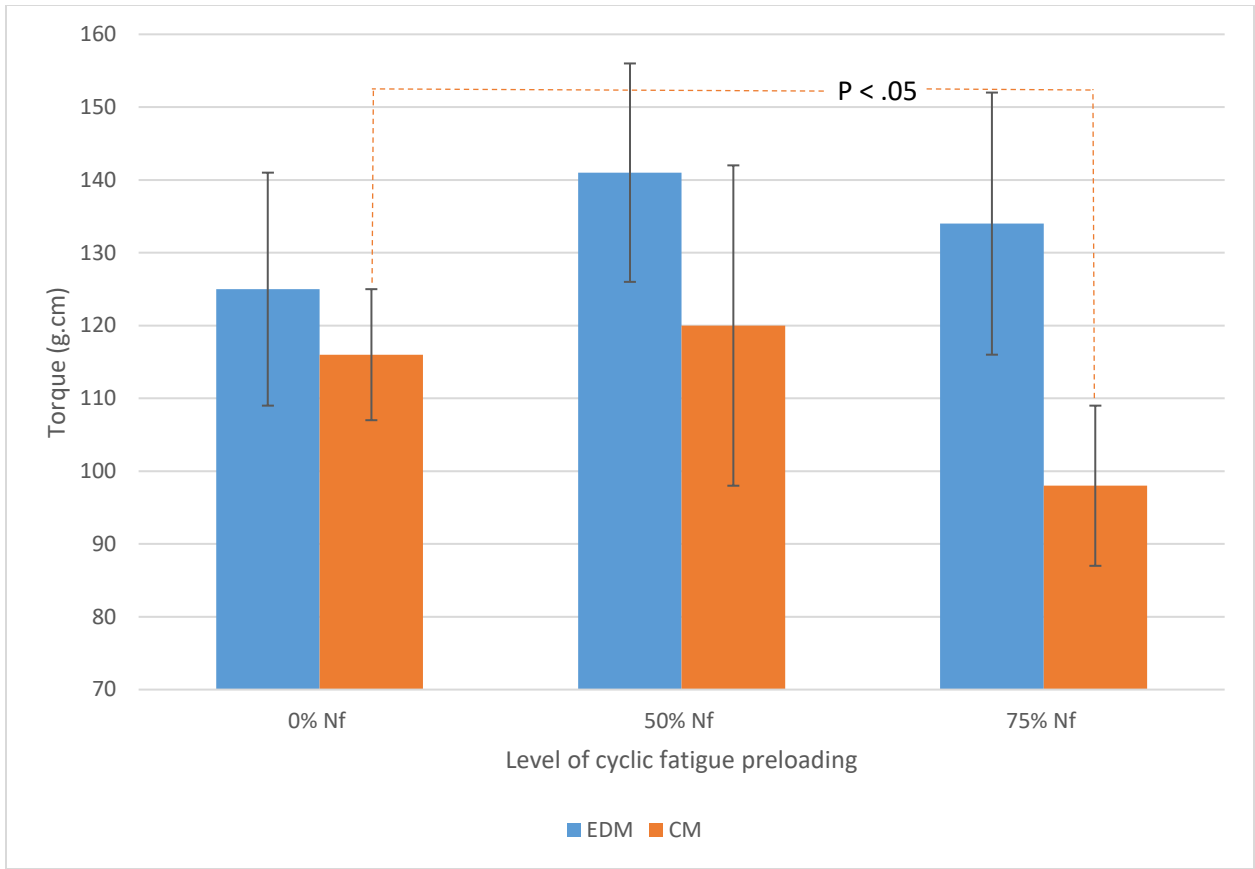


Figure 13 - Torque (g·cm) at torsional fracture after different levels of cyclic fatigue preloading.

### 3.3 Effect of torsional preloading on cyclic fatigue resistance

In the torsional preloading groups, 15% of torsional preloading significantly reduced the mean  $N_f$  of HyFlex EDM files ( $P < .05$ ) (Table 6, Figure 14), while a moderate amount of 50% torsional preloading significantly lowered the  $N_f$  of HyFlex CM files ( $P < .05$ ) (Table 6, Figure 14). However, the  $N_f$  of HyFlex EDM files even with 50% torsional preloading was still significantly higher than the  $N_f$  of HyFlex CM files without any torsional preloading ( $P < .05$ ) (Table 6, Figure 14).

Table 6 -  $N_f$  (rotations  $\pm$  SD) after preloading with different levels of torsional pre-stress.

|     | 0% $\Theta$    | 5% $\Theta$    | 15% $\Theta$   | 25% $\Theta$   | 50% $\Theta$   |
|-----|----------------|----------------|----------------|----------------|----------------|
| EDM | 2490 $\pm$ 306 | 2208 $\pm$ 331 | 1959 $\pm$ 412 | 1891 $\pm$ 309 | 1653 $\pm$ 191 |
| CM  | 1029 $\pm$ 158 | 841 $\pm$ 164  | 768 $\pm$ 177  | 833 $\pm$ 246  | 588 $\pm$ 177  |

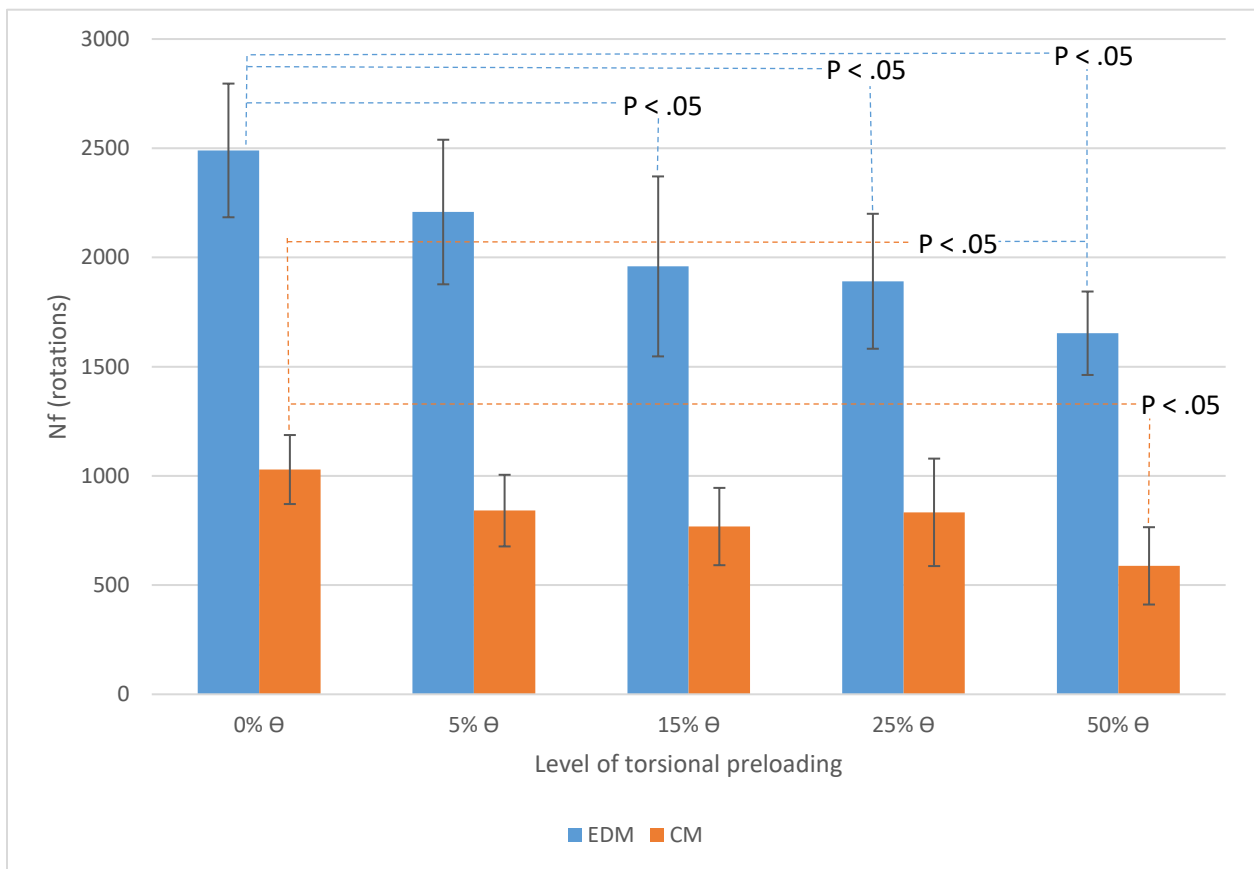


Figure 14 -  $N_f$  (rotations) after preloading with different levels of torsional angle.

### 3.4 SEM images

A close-up SEM view of the HyFlex EDM files showed the presence of a peculiar irregular surface texture derived from the manufacturing process. High-magnification

micrographs disclosed a non-uniform crater-like surface where pits, pores and voids were observed on a 'rough spark-machined' surface (Figure 15). In comparison, the HyFlex CM files presented a smooth machined surface without any surface irregularities (Figure 16). Multiple microcracks were visible running perpendicularly to the longitudinal axis of a pure fatigue fractured HyFlex CM file (Figure 16). There was no apparent unwinding of the flutes for the files fractured by fatigue stress only; this was true for both file systems. The fracture surface for these files showed the typical pattern of cyclic fatigue fracture: a crack origin, an area showing microscopic fatigue striations and a dimple rupture could be identified on all fracture surfaces (Figures 17, 18).

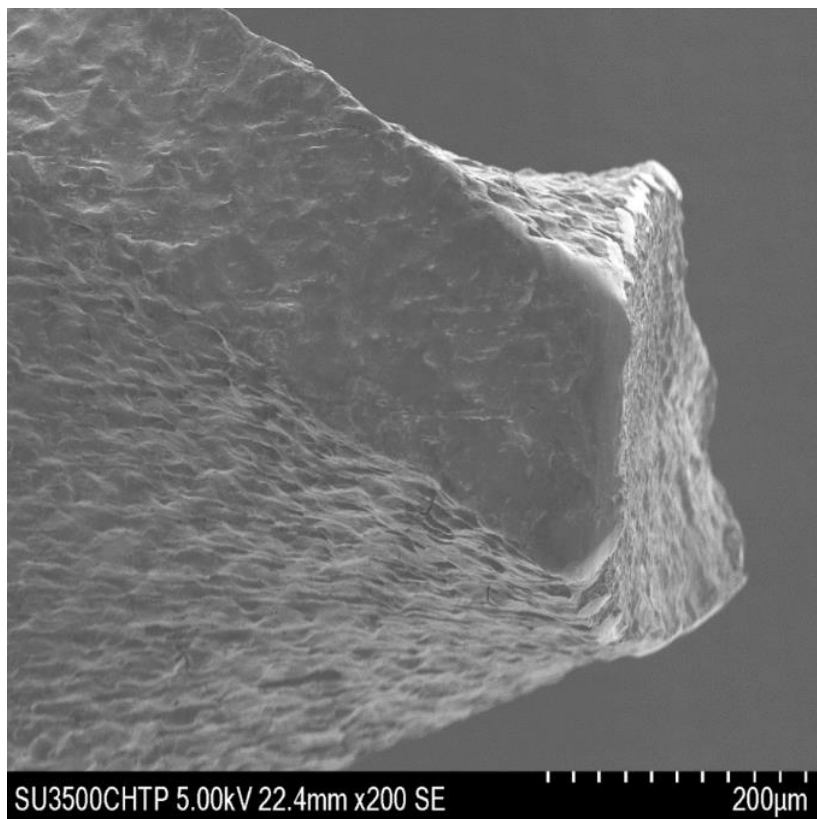


Figure 15 - Longitudinal view of a fractured HyFlex EDM by cyclic fatigue stress only.

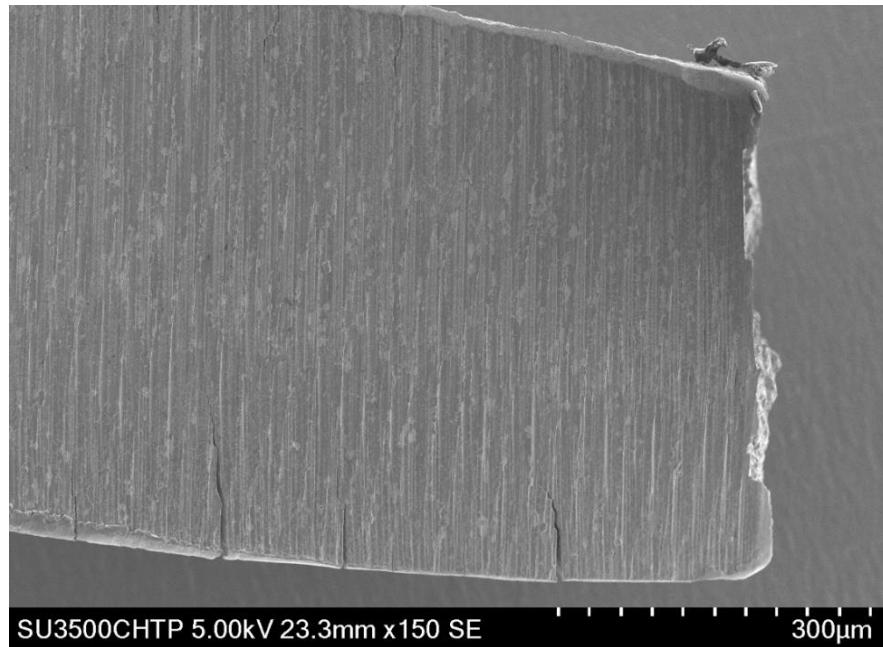


Figure 16 - Longitudinal view of a fractured HyFlex CM by cyclic fatigue stress only.

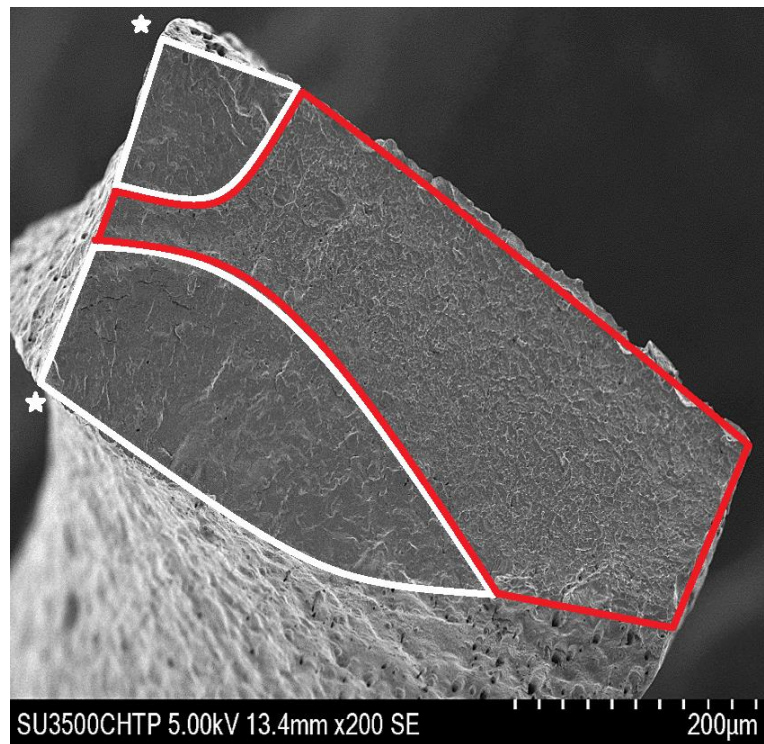


Figure 17 - Fractured surface of HyFlex EDM by cyclic fatigue stress only showing multiple crack origins (asterisk), an area showing microscopic fatigue striations (white outline) and a dimple rupture (red outline).

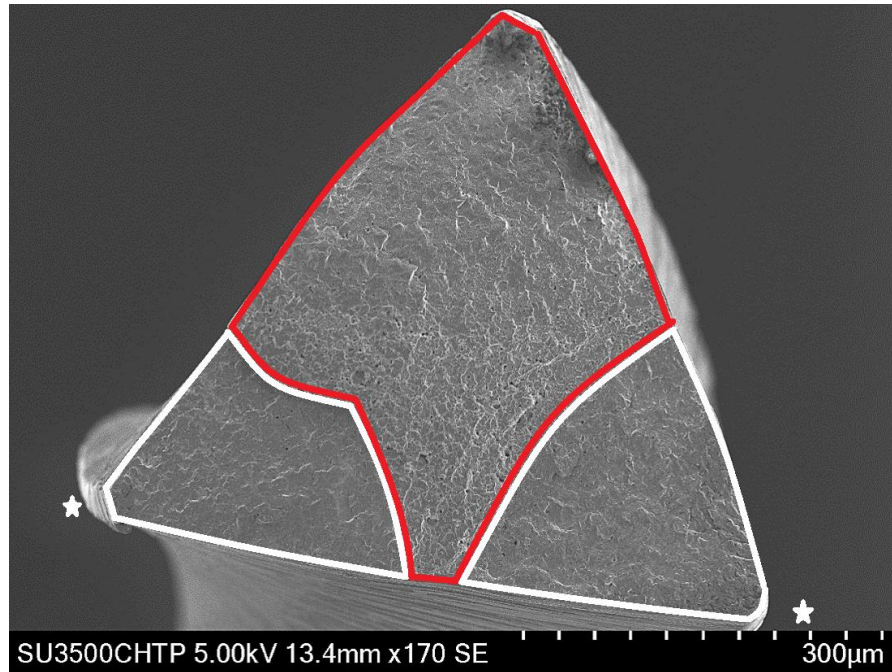


Figure 18 - Fractured surface of HyFlex CM by cyclic fatigue stress only showing multiple crack origins (asterisk), an area showing microscopic fatigue striations (white outline) and a dimple rupture (red outline).

HyFlex EDM and HyFlex CM files fractured by pure torsional stress showed unwinding on the longitudinal view (Figures 19, 23). The fractured surface (Figures 20, 24) of these files showed circular abrasion marks (Figures 21, 25), no fatigue striations and a centered area of skewed dimples (Figures 22, 26).



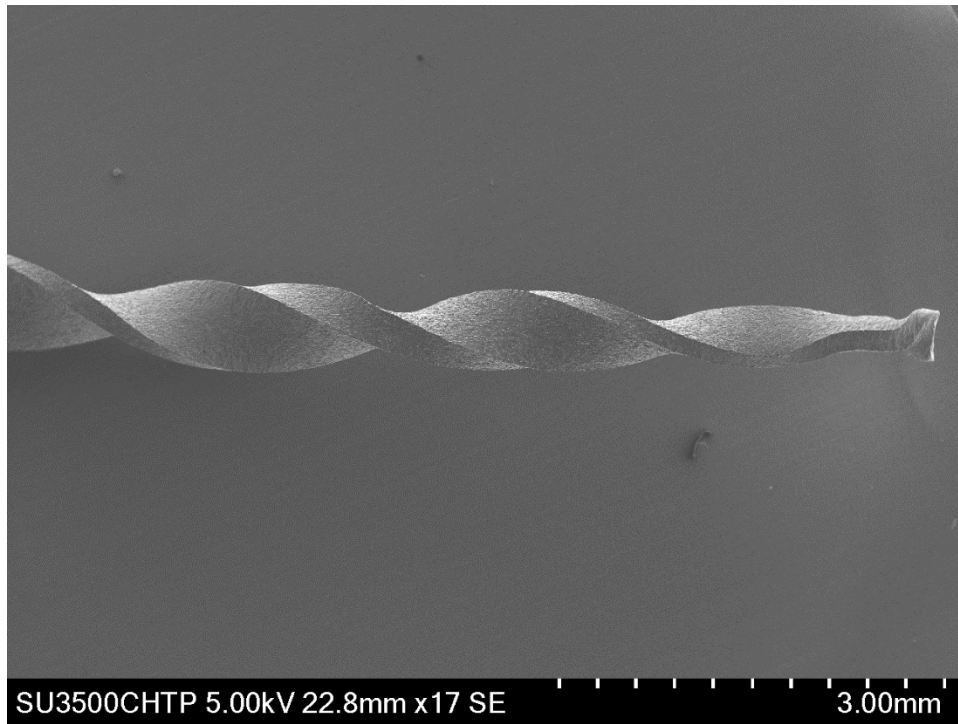


Figure 19 - Unwinding of a HyFlex EDM file after pure torsional fracture.

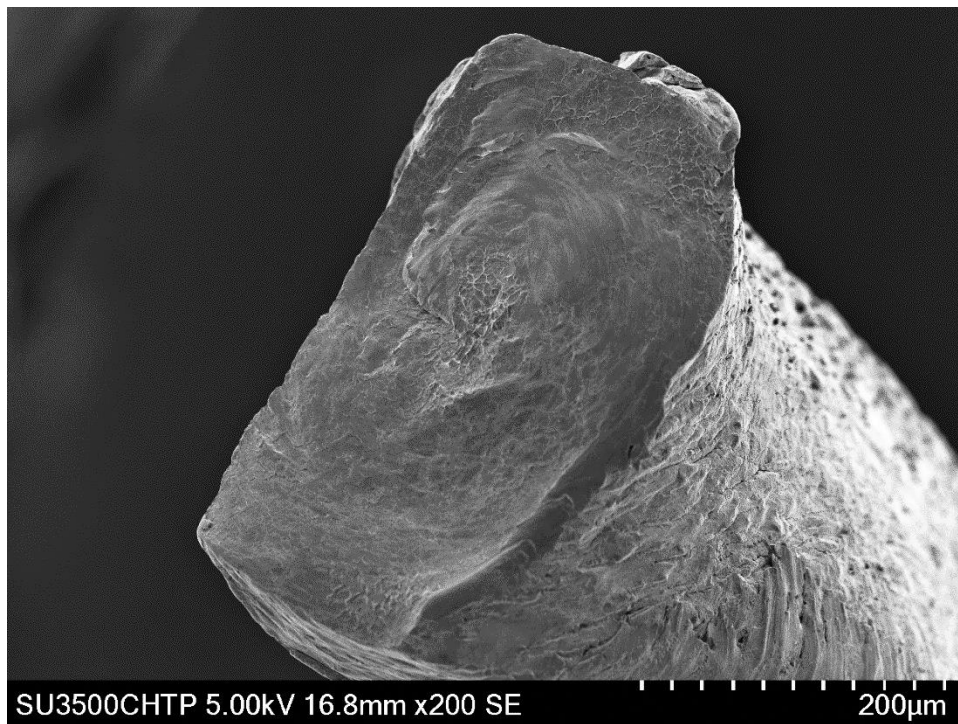


Figure 20 - Fractured surface of HyFlex EDM file after pure torsional fracture showing circular abrasion marks, no fatigue striations and a centered area of skewed dimples.



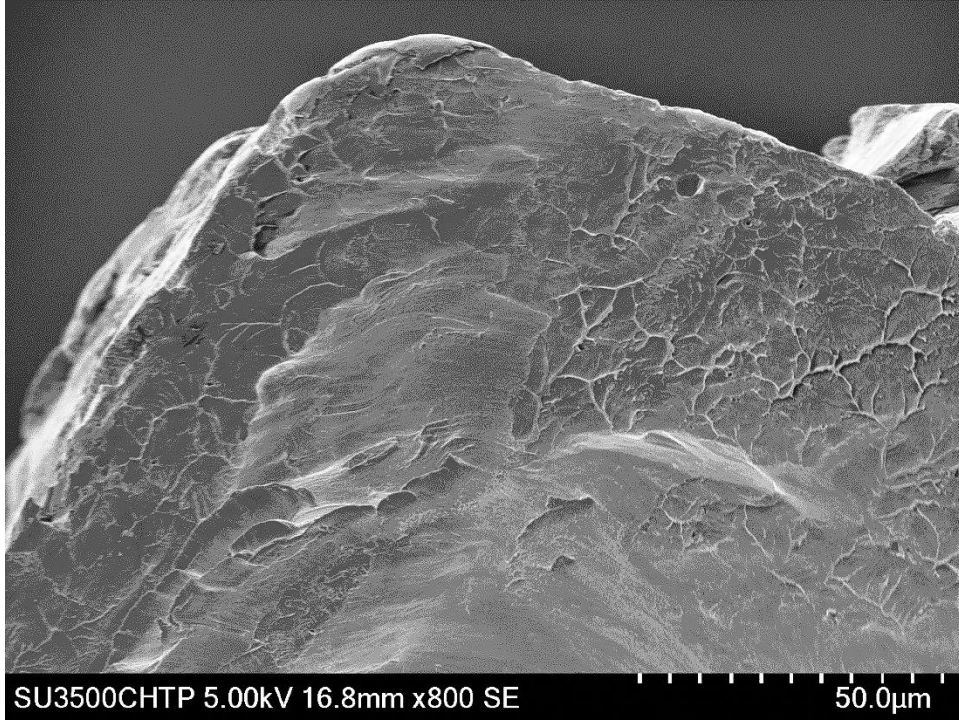


Figure 21 - A close-up image of circular abrasion marks from picture in Figure 20.

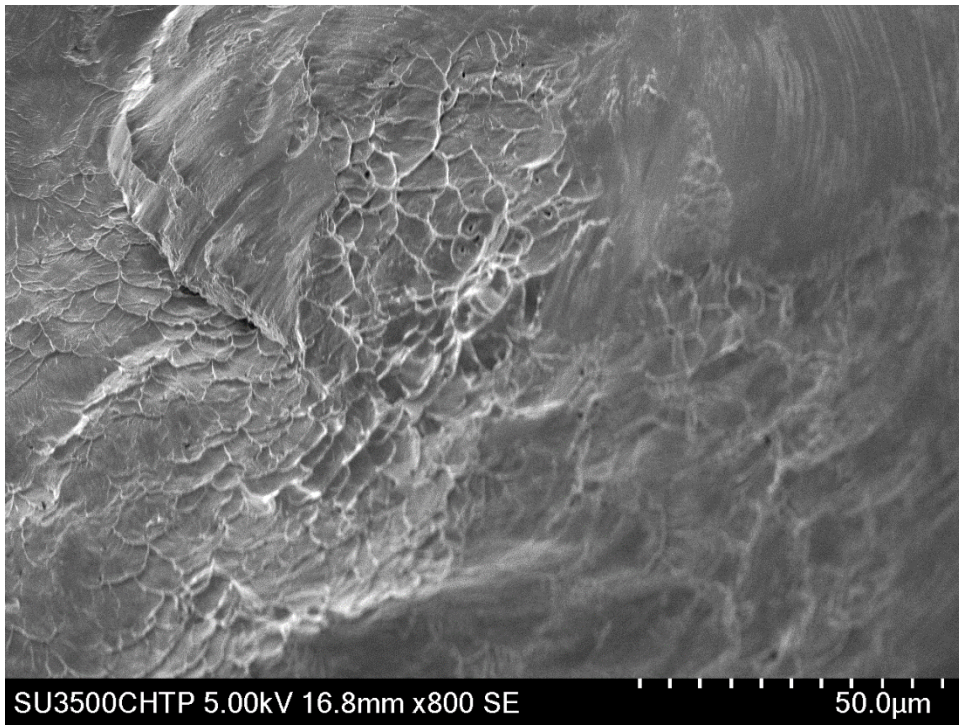


Figure 22 - A close-up image of skewed dimples at the center area from Figure 20.

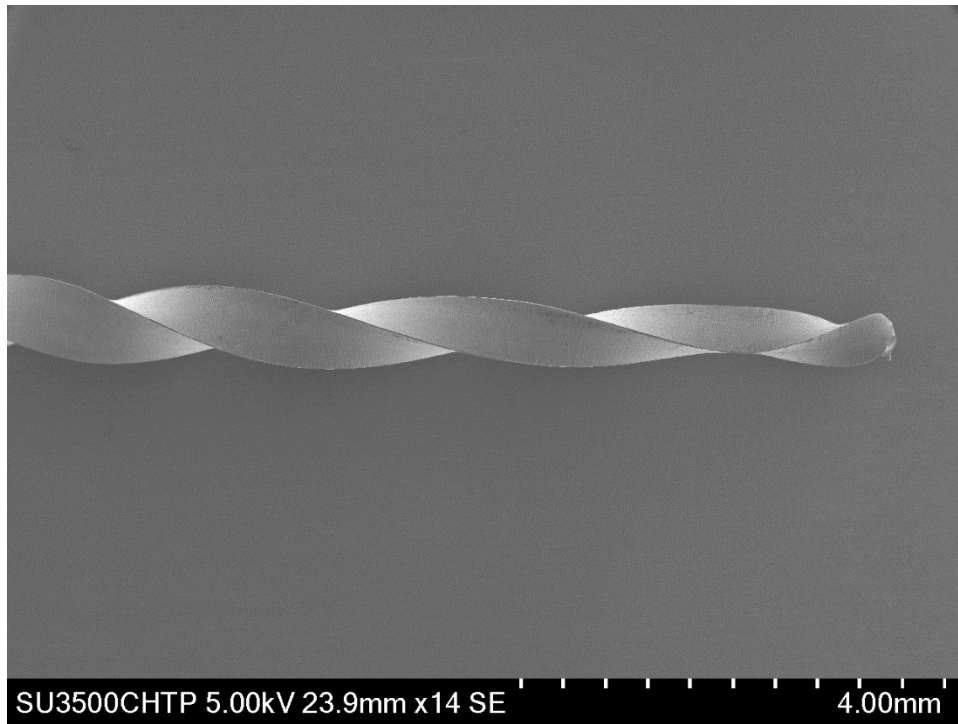


Figure 23 - Unwinding of a HyFlex CM file after pure torsional fracture.

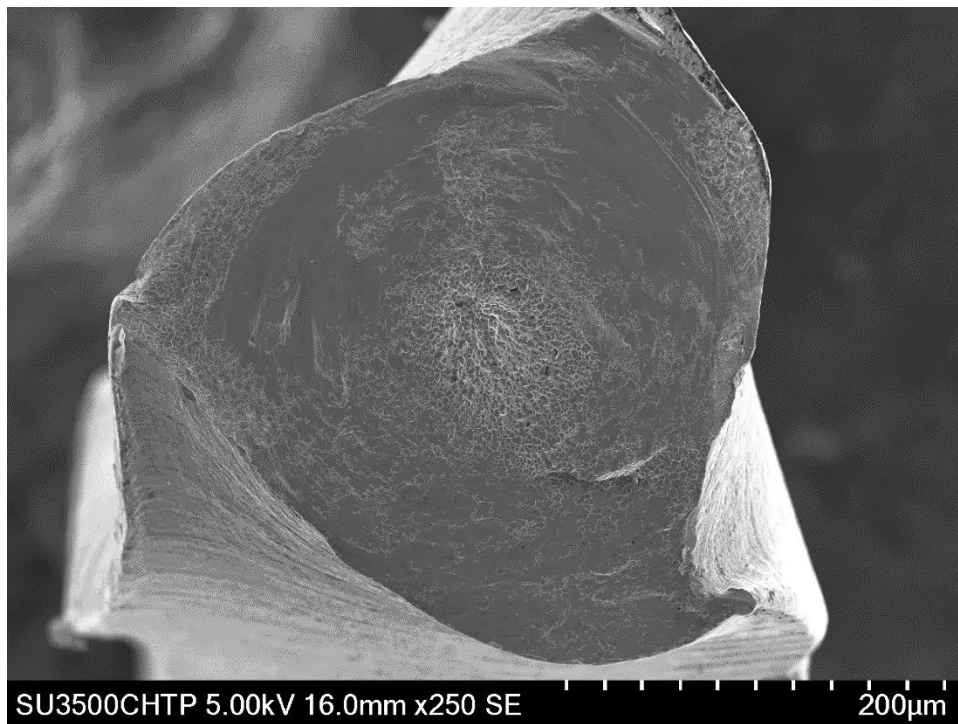


Figure 24 - Fractured surface of HyFlex CM file after pure torsional fracture.



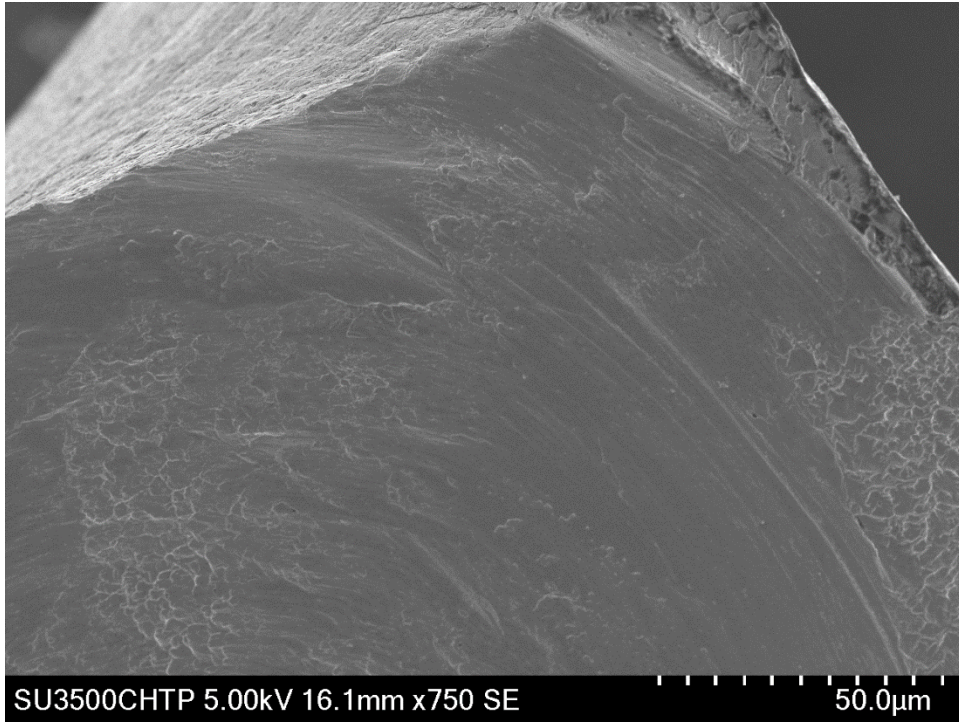


Figure 25 - A close-up image of circular abrasion marks from picture in Figure 24.

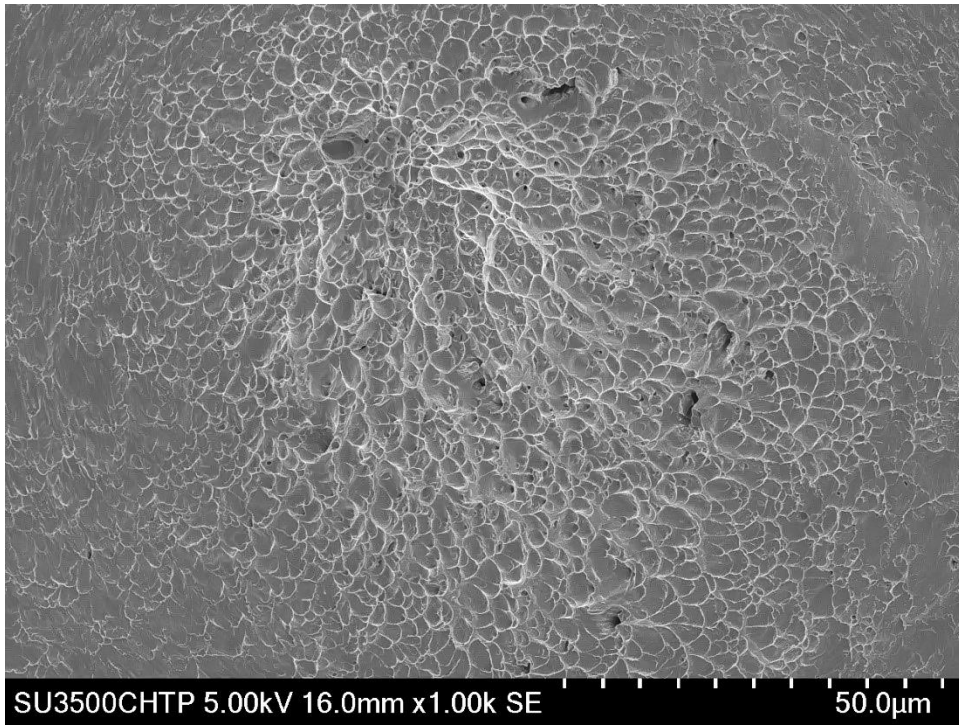


Figure 26 - A close-up image of skewed dimples at the center area in Figure 24.

After 15% torsional preloading, both HyFlex EDM (Figure 27) and HyFlex CM (Figure 29) files showed microcracks about 3-4 mm away from the fracture line. The microcracks ran irregularly perpendicular to the longitudinal axis of the file close to the fractured area. When the instruments failed by cyclic fatigue after a preloading of torsional stress, the fractography showed similar appearance as the surface of a file fractured by pure cyclic fatigue stress, i.e. a crack origin, fatigue striations and a dimple rupture area (Figure 28, 30). Most of the pure cyclic fatigue fractured HyFlex EDM and HyFlex CM files had multiple crack origins, which were usually located at the cutting edges or flat edges (Figure 17, 18). The length of the fractured piece was ca. 4 mm after fatigue failure. In the same manner, HyFlex EDM and HyFlex CM files fractured by torsional stress with or without cyclic fatigue preloading showed the characteristic fracture surface of a torsional fracture (Figure 31, 32). Thus, fractography analysis revealed a fractured surface typical to the nature of the last type of stress applied to the file.



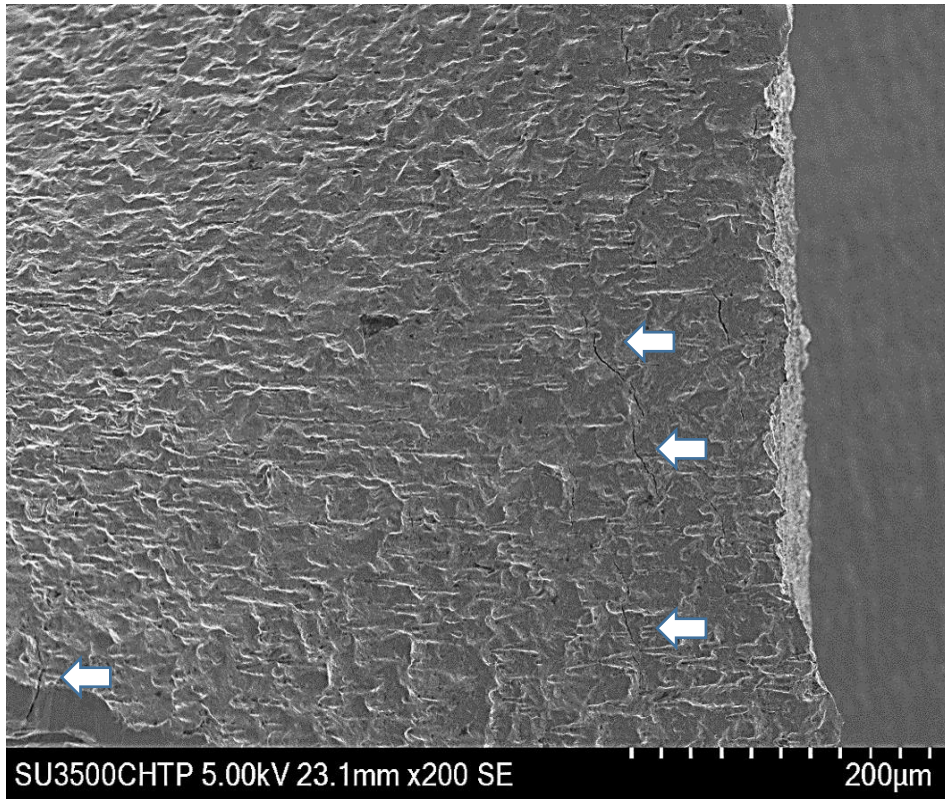


Figure 27 - Microcracks visible (arrows) on the surface of a HyFlex EDM file fractured due to cyclic fatigue after 15% torsional preloading.

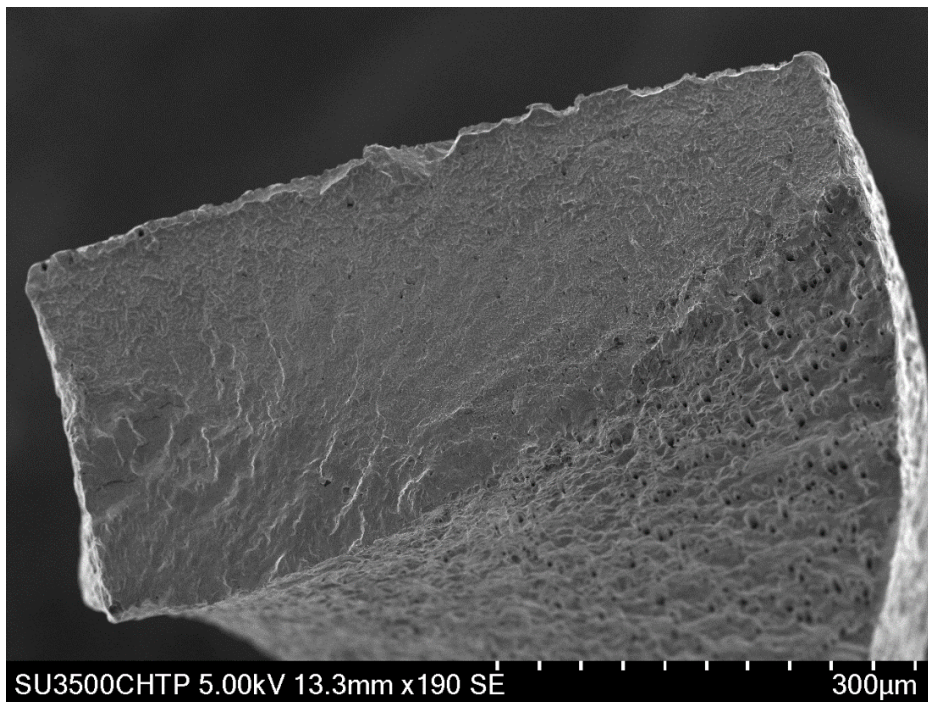


Figure 28 - Fractured surface of a HyFlex EDM file after 15% torsional preloading and failure by cyclic fatigue.

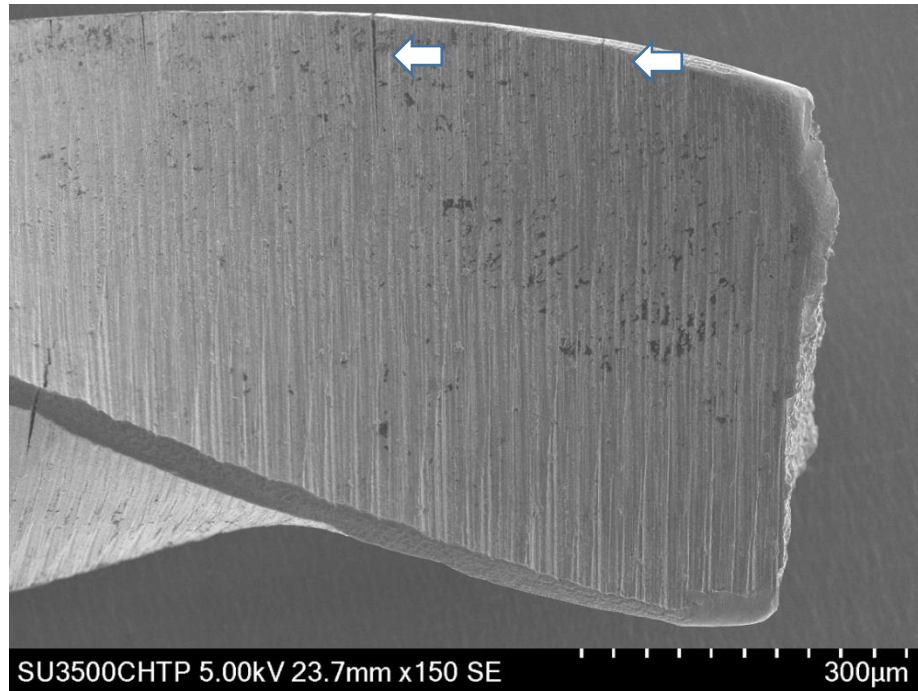


Figure 29 - Microcracks visible (arrows) on the surface of a HyFlex CM file fractured due to cyclic fatigue after 15% torsional preloading.

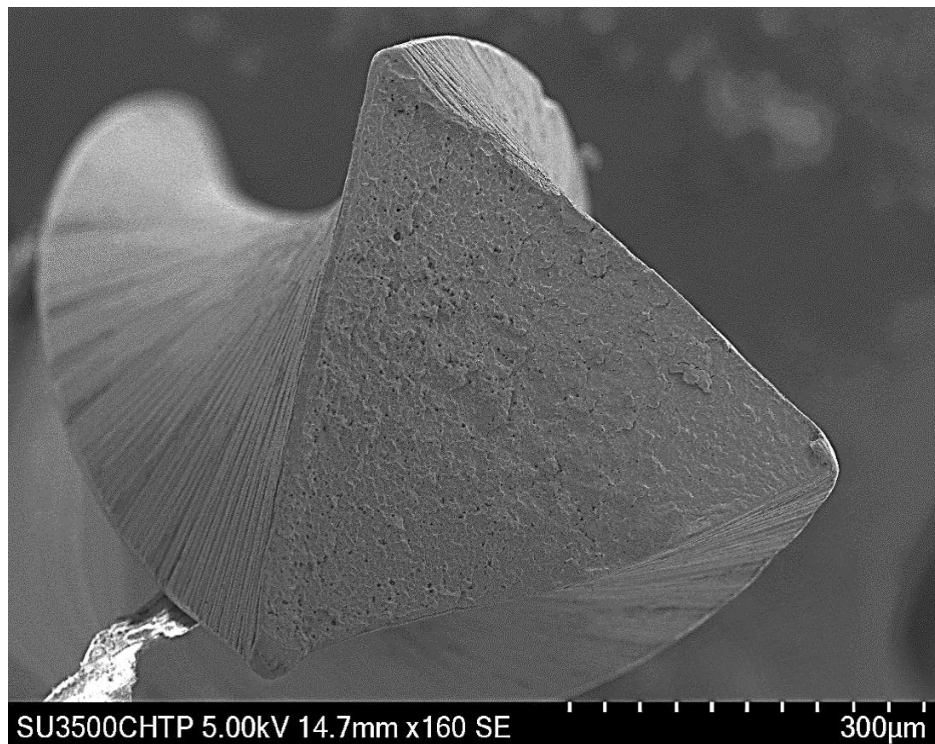


Figure 30 - Fractured surface of a HyFlex CM file after 15% torsional preloading and failure by cyclic fatigue.



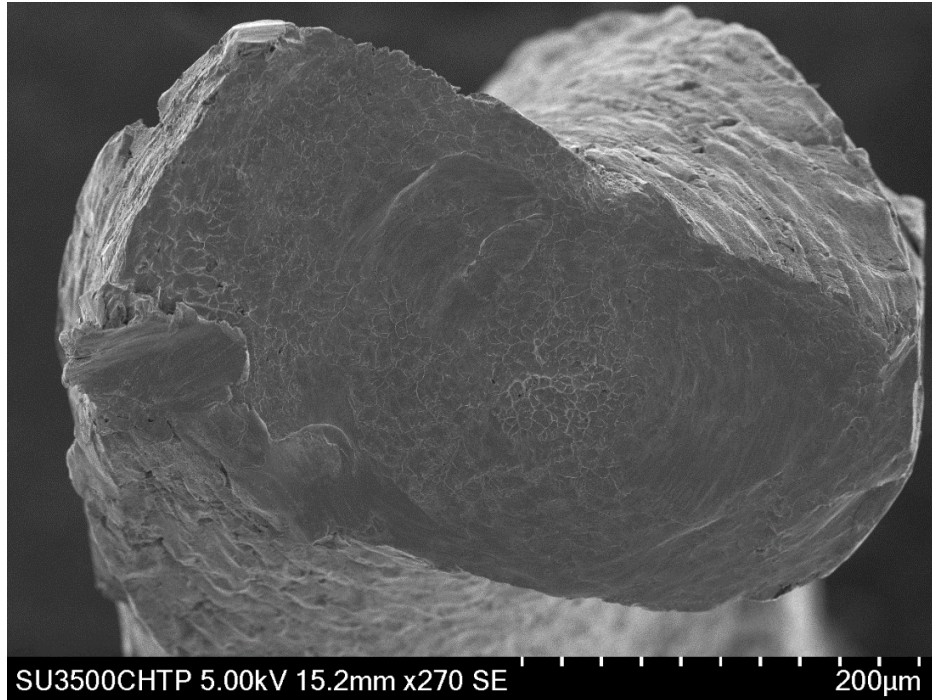


Figure 31 - Fractured surface of a HyFlex EDM file after 75% fatigue preloading and failure by shear stress.

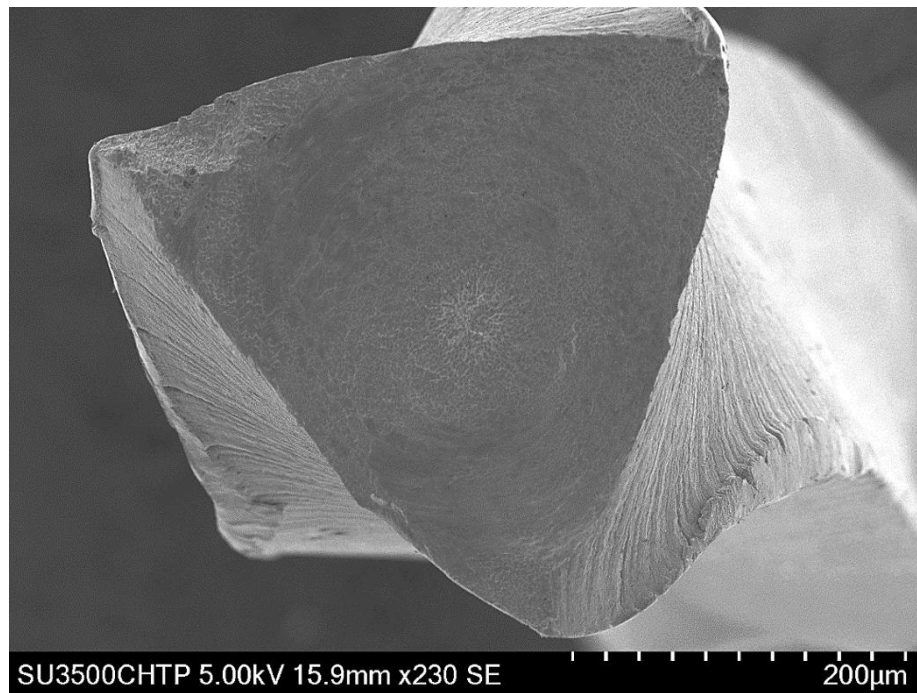


Figure 32 - Fractured surface of a HyFlex CM file after 50% fatigue preloading and failure by shear stress.

## Chapter 4: Discussion

### 4.1 HyFlex EDM

Despite the fact that a fractured file does not affect the outcome of endodontic treatment (Spili et al, 2005), a clinician would rather avoid this clinical mishap because it would make the work more difficult and could cause a loss of confidence by the patient or a referring dentist. Manufacturers continuously launch new files with innovative designs and improved metallurgy while promoting the superiority of their new files regarding efficiency and safety. HyFlex EDM is a novel type of file developed by Coltene/Whaledent, introduced in February 2016. It is made from the same thermally improved CM NiTi alloy as the HyFlex CM. The main feature of the HyFlex EDM is its manufacturing process: the file is fabricated by electrical discharge machining (EDM) process. This creates a 'rough spark-machined' surface characterized by craters, pits, pores and voids. The EDM process uses sparks to melt and evaporate the surface of the alloy to give its final shape. As per the manufacturer's claims, it results with a harder surface with better cutting efficiency and with less risk of fracture. Another advantage from this unique manufacturing process is the ability to create a complex cross-sectional file design: from a rectangular cross-section at the tip, the file gradually changes to an almost triangular cross-section near the shank of the file. This supposedly increases the file's resistance to fracture by increasing the cross-sectional surface at the tip where torsional stress is more likely to occur, and by having a triangular cross-section at the higher portion of the file, which is more able to sustain flexural stress.

Benchmark laboratory tests are necessary to verify these claims and to understand the clinical behavior of the files. Thus, the clinician can decide which file system to choose for



endodontic treatments and which is the most optimal manner to use it to avoid clinical mishaps such as transportation and file fracture. Fracture resistance of endodontic files have been mostly studied by examining the two modes of fractures separately. However, endodontic files are subjected to a simultaneous effect of torsional and cyclic fatigue stresses during their clinical use. However, at the present, no test can fully replicate the clinical conditions present during the use of the endodontic file. This study attempted to get one step closer to the real situation by combining both torsional and cyclic fatigue factors in the study of the fracture resistance of HyFlex EDM file.

#### **4.2 Fatigue life of HyFlex EDM**

The results of our study showed that HyFlex EDM files had a higher cyclic fatigue resistance than HyFlex CM files ( $P < .05$ ). The mean number of rotations before cyclic fatigue fracture was almost 150% higher than that of HyFlex CM files. The difference in the cross-section of the file and the presence of the 'EDM surface' could explain the increase in resistance to cyclic fatigue. However, another reason could be found in the metallurgical characteristics of the HyFlex EDM file. Despite the fact that both HyFlex EDM and HyFlex CM files are made from the same CM wire, the relative proportions and characteristics of the NiTi microstructural phases of HyFlex EDM differ from the HyFlex CM. Iacono et al (2017) characterized the phase composition and examined the structure of HyFlex EDM and HyFlex CM with the aids of x-ray diffraction techniques and differential scanning calorimetry (DSC). X-ray diffraction is a technique used to identify the crystallite structure of NiTi (Shen and Cheung, 2013). Phase transformation either from martensite to austenite or to the opposite direction is accompanied by an endothermic reaction for the former and an exothermic for the

latter. The peaks in the temperature change can be detected by DSC when the NiTi alloy is heated or cooled down. Therefore, DSC reveals the transformation temperature range (phase transformation temperature) of the alloy, thus characterizing the crystallite phase of NiTi at room temperature (Shen and Cheung, 2013). Iacano et al (2017) showed that x-ray diffraction had higher presence of martensitic phase and intermediary R-phase in the HyFlex EDM files compared to the HyFlex CM files. HyFlex CM files showed higher amount of austenite, lower amount of martensite and small amount of R-phase (Iacono et al, 2017). Martensite and R-phase render the alloy more ductile. Also, in the same study, DSC analysis also revealed a higher phase transformation temperature from martensite to austenite for HyFlex EDM files ( $51-54^{\circ}\text{C}$ ) than for HyFlex CM files ( $32-37^{\circ}\text{C}$ ) (Iacono et al, 2017). Consequently, the higher contents in martensite and R-phase of the HyFlex EDM could explain its better cyclic fatigue resistance compared to HyFlex CM. Pirani et al (2016) also found improved cyclic fatigue resistance of HyFlex EDM when compared to HyFlex CM. They found that the fatigue life of HyFlex EDM files was up to six times higher than HyFlex CM files (Pirani et al, 2016). The difference between the present study and the Pirani study may be the different fatigue modes used: customized canal (size #40, taper 0.06) vs. heat bent 16-G stainless steel needle.

### **4.3 Torsional resistance of HyFlex EDM files**

In the present study, there was no significant difference between the torsional load and the distortion angle at fracture of unused HyFlex EDM files and unused HyFlex CM files. Our results showed that the HyFlex EDM files had a mean torsional load of  $125 \pm 16$  g.cm and a mean distortion angle of  $797 \pm 57^{\circ}$  at fracture. For comparison purposes, Pedullà et al (2016) reported the corresponding values as  $135.6 \pm 5.1$  g.cm ( $1.33 \pm 0.05$  N.cm) and  $536.20 \pm 96.70^{\circ}$ .

Other studies found no difference in the torsional load and distortion angle at fracture between the heat-treated K3XF file and its counterpart made from conventional superelastic NiTi, the K3 file (Ha et al, 2013; Shen et al, 2015). Therefore, it seems that thermally modified metallurgy does not bring gain in torsional resistance of the NiTi, neither does it weaken it.

#### **4.4 Effect of cyclic fatigue preloading on the torsional resistance of HyFlex EDM**

Recently, a couple of studies found that cyclic fatigue was not detrimental to the ability of heat-treated files, such as K3XF files and Typhoon CM files in size #25, 0.04 taper to withstand torsional load (Campbell et al, 2014; Shen et al, 2015). This is in agreement with our results that cyclic fatigue had no effect on the torsional fracture resistance of HyFlex EDM files. Interestingly, the group of HyFlex EDM files with 50% of cyclic fatigue preloading showed slight increase in the maximum torsional load and distortion angle at fracture, although this was statistically insignificant. It is unclear what the reasons for this effect are. This result suggests that even a high amount of cyclic fatigue preloading would not be detrimental to ability of HyFlex EDM file to withstand torsional load. A high angle of rotation before the fracture of HyFlex EDM files may be beneficial because it may provide an indication to clinicians that there is a permanent plastic deformation and a fracture may be imminent if the file is continued to be used.

In our experiment, cyclic fatigue preloading did, however, affect the torsional resistance of HyFlex CM files by decreasing the distortion angle at fracture after 50% of cyclic fatigue preloading, and the torsional load after 75% cyclic fatigue preloading. The novel file surface and rectangular cross-section of HyFlex EDM files could explain the non-influence of cyclic fatigue preloading on torsional resistance in comparison with HyFlex CM files.

#### **4.5 Effect of torsional preloading on the fatigue life of HyFlex EDM**

The effect of torsional preloading on the cyclic fatigue resistance has been studied in conventional NiTi files and heat-treated NiTi files (Barbosa et al, 2007; Bahia et al, 2008; Cheung et al, 2013; Shen et al, 2015; Pedullà et al, 2015). Previous studies have shown that torsional preloading reduced the fatigue resistance of conventional NiTi files (Barbosa et al, 2007; Bahia et al, 2008) and heat-treated K3XF files (Shen et al, 2015). Pedullà et al (2015) found that 50% and 75% torsional preloading significantly reduced the fatigue resistance of HyFlex CM files (size #25, taper 0.06). It is not easy to determine how much torsional preloading may affect the fatigue life of the files. During the pilot experiments, it was noticed that even 15% torsional preloading reduced the fatigue resistance of HyFlex EDM files. Therefore, to obtain sufficient information, the lowest amount of torsional preloading by both files started from 5% preloading. Our results showed that the fatigue life of both types of files reduced even with very low (5%) torsional preloading, although there was no statistical difference between files with and without 5% preloading. The fatigue life of HyFlex EDM was significantly affected after 15% of torsional preloading, and HyFlex CM, after 50% preloading. This behavior is probably associated with the generation of surface defects during torsional loading cycles, which can act as crack nucleation sites for flexural fatigue fracture. Interestingly, the fatigue life of HyFlex EDM files with even 50% torsional preloading was still longer than the fatigue life of HyFlex CM files without any torsional preloading. In the clinical situation, there is no simple way to estimate the amount of torsional stress accumulated in instruments used in multiple canals or teeth. During the early stage of canal enlargement, the file is likely to be exposed to greater torsional stresses from contacts with the canal, more than to cyclic fatigue, especially when it is used in a narrow and constricted canal. Thus, it

would seem advisable that during the creation of a glide path one avoids the so-called screw-in effect or taper lock effect that may occur when the canal cross section is smaller than the tip of the instrument (Peters et al, 2003; Arias et al, 2017). Another clinical implication deriving from this study could be the suggestion to start instrumenting larger canals before smaller canals in multi-rooted teeth, thus reducing the exposure to torsional stresses in the early stages. Because files are sterilized and reused by many dentists, it would be wise to discard a file used in a very narrow canal (e.g. calcified canal) to avoid potential future risk of instrument fracture. Otherwise, if used in a subsequent root canal treatment, the file which was subjected to high level of torsional preloading would be more prone to a flexural fatigue fracture.

HyFlex EDM files performed much better in all cyclic fatigue testing compared to HyFlex CM files. Interestingly, the cross-section of a fractured HyFlex EDM (Figure 17, 28) file by cyclic fatigue was rectangular compared to the triangular cross-section of a fractured HyFlex CM file (Figure 18, 30). This goes against the normal findings where the increased surface area associated with a rectangular cross-section is less resistant to flexural fatigue stress than a triangular cross-section (Iqbal et al, 2006). Therefore, we speculate that the crater-like surface created by the EDM manufacturing process contributes to the increase in the cyclic fatigue resistance of the HyFlex EDM.

## Chapter 5: Conclusion

In conclusion, under the experimental conditions, the fracture resistance of the HyFlex EDM files showed the following characteristics:

1. HyFlex EDM showed a higher cyclic fatigue resistance, but a similar torsional resistance, compared to HyFlex CM.
2. A cyclic fatigue preloading did not affect the torsional resistance of HyFlex EDM.
3. The cyclic fatigue resistance was negatively affected by as low as 15% torsional preloading.
4. The SEM images of the fractured surface showed fractographic patterns consistent with the last mode of stress applied to the instrument (torsional or cyclic fatigue).

Laboratory tests are never able to totally replicate clinical conditions associated with the use of endodontic files because of its multifactorial nature. Nevertheless, the results of this study could improve the understanding of the dynamics of file fracture and could guide the clinician for a safer clinical use of this novel, promising file. The avoidance of the screw-in effect or taper lock, the awareness to reduce torsional stress to the file in the early stage of the instrumentation and the understanding of a weakened file after its use in a calcified canal, are examples of clinical implications derived from our study. Innovations in file fabrication and design lead to more efficient and safer endodontic treatments.

## **Bibliography**

Ankrum MT, Hartwell GR, Truitt JE. K3 Endo, ProTaper, and ProFile systems: breakage and distortion in severely curved roots of molars. *J Endod* 2004;30(4):234-237.

Arias A, de Vasconcelos RA, Hernández A, Peters OA. Torsional performance of ProTaper Gold rotary instruments during shaping of small root canals after 2 different glide path preparations. *J Endod* 2017;43(3):447-51.

Bahia MG, Melo MC, Buono VT. Influence of cyclic torsional loading on the fatigue resistance of K3 instruments. *Int Endod J* 2008;41(10):883-91.

Barbosa FOG, Gomes JA, de Araújo MC. Influence of previous angular deformation on flexural fatigue resistance of K3 nickel–titanium rotary instruments. *J Endod* 2007;33(12):1477-80.

Bergenholtz G, Lekholm U, Milthon R, Heden G, Ödesö B, Engström B. Retreatment of endodontic fillings. *Eur J Oral Sci* 1979;87(3):217-24.

Buehler WJ, Gilfrich JV, Wiley RC. Effect of low-temperature phase changes on the mechanical properties of alloys near composition TiNi. *J Appl Phys* 1963;34(5):1475-7.

Campbell L, Shen Y, Zhou HM, Haapasalo M. Effect of fatigue on torsional failure of nickel-titanium controlled memory instruments. *J Endod* 2014;40(4):562-5.

Cheung GS, Oh SH, Ha JH, Kim SK, Park SH, Kim HC. Effect of torsional loading of nickel-titanium instruments on cyclic fatigue resistance. *J Endod* 2013;39(12):1593-7.

Cheung GS, Peng B, Bian Z, Shen Y, Darvell BW. Defects in ProTaper S1 instruments after clinical use: fractographic examination. *Int Endod J* 2005;38(11):802-9.

DesRoches R, McCormick J, Delemont M. Cyclic properties of superelastic shape memory alloy wires and bars. *J Struct Eng* 2004;130(1):38-46.

Friedman S, Stabholz A. Endodontic retreatment—case selection and technique. Part 1: Criteria for case selection. *J Endod* 1986;12(1):28-33.

Gambill JM, Alder M, Carlos E. Comparison of nickel-titanium and stainless steel hand-file instrumentation using computed tomography. *J Endod* 1996;22(7):369-75.

Glosson CR, Haller RH, Dove SB, Carlos E. A comparison of root canal preparations using Ni-Ti hand, Ni-Ti engine-driven, and K-Flex endodontic instruments. *J Endod* 1995;21(3):146-51.



Gluskin AH, Brown DC, Buchanan LS. A reconstructed computerized tomographic comparison of Ni-Ti rotary GT™ files versus traditional instruments in canals shaped by novice operators. *Int Endod J* 2001;34(6):476-84.

Grossman LI. Guidelines for the prevention of fracture of root canal instruments. *Oral Surg Oral Med Oral Pathol* 1969;28(5):746-52.

Günday M, Sazak H, Garip Y. A comparative study of three different root canal curvature measurement techniques and measuring the canal access angle in curved canals. *J Endod* 2005;31(11):796-8.

Ha JH, Kim SK, Cohenca N, Kim HC. Effect of R-phase heat treatment on torsional resistance and cyclic fatigue fracture. *J Endod* 2013;39(3):389-93.

Haapasalo M, Shen Y. Evolution of nickel-titanium instruments: from past to future. *Endod Topics* 2013;29(1):3-17.

Hankins PJ, ElDeeb ME. An evaluation of the canal master, balanced-force, and step-back techniques. *J Endod* 1996;22(3):123-30.

HyFlex EDM brochure (2016), Coltene/Whaledent, Inc. Available at: [https://nam.coltene.com/products/endodontics/rotary-files/hyflex-rotary-files/hyflex™-edm-niti-files/](https://nam.coltene.com/products/endodontics/rotary-files/hyflex-rotary-files/hyflexTM-edm-niti-files/) . Accessed on Dec 2, 2016.

Iacono F, Pirani C, Generali L, Bolelli G, Sassatelli P, Lusvarghi L, Gandolfi MG, Giorgini L, Prati C. Structural analysis of HyFlex EDM instruments. *Int Endod J* 2017;50(3):303-13.

Iqbal MK, Kohli MR, Kim JS. A retrospective clinical study of incidence of root canal instrument separation in an endodontics graduate program: a PennEndo database study. *J Endod* 2006;32(11):1048-52.

Jameson EC. *Electrical discharge machining*. Dearborn: Society of Manufacturing Engineers;2001.

Takehashi S, Stanley HR, Fitzgerald RJ. The effects of surgical exposures of dental pulps in germ-free and conventional laboratory rats. *Oral Surg Oral Med Oral Pathol* 1965;20(3):340-9.

Kim JY, Cheung GS, Park SH, Ko DC, Kim JW, Kim HC. Effect from cyclic fatigue of nickel-titanium rotary files on torsional resistance. *J Endod* 2012;38(4):527-30.

Metzger Z, Solomonov M, Kfir A. The role of mechanical instrumentation in the cleaning of root canals. *Endod Topics* 2013;29(1):87-109.

Ørstavik D, Pitt Ford TR. *Apical periodontitis: microbial infection and host responses. Essential endodontology. Prevention and treatment of apical periodontitis*. Oxford: Blackwell Science;1998.

Parashos P, Gordon I, Messer HH. Factors influencing defects of rotary nickel-titanium endodontic instruments after clinical use. *J Endod* 2004;30(10):722-5.

Pedullà E, Savio FL, Boninelli S, Plotino G, Grande NM, Rapisarda E, La Rosa G. Influence of cyclic torsional preloading on cyclic fatigue resistance of nickel–titanium instruments. *Int Endod J* 2015;48(11):1043-50.

Pedullà E, Savio FL, Boninelli S, Plotino G, Grande NM, La Rosa G, Rapisarda E. Torsional and cyclic fatigue resistance of a new nickel-titanium instrument manufactured by electrical discharge machining. *J Endod* 2016;42(1):156-9.

Peng B, Shen Y, Cheung GS, Xia TJ. Defects in ProTaper S1 instruments after clinical use: longitudinal examination. *Int Endod J* 2005;38(8):550-7.

Peters OA, Peters CI, Schönenberger K, Barbakow F. ProTaper rotary root canal preparation: assessment of torque and force in relation to canal anatomy. *Int Endod J* 2003;36(2):93-9.

Pirani C, Iacono F, Generali L, Sassatelli P, Nucci C, Lusvarghi L, Gandolfi MG, Prati C. HyFlex EDM: superficial features, metallurgical analysis and fatigue resistance of innovative electro discharge machined NiTi rotary instruments. *Int Endod J* 2016;49:483-93.

Plotino G, Grande NM, Cordaro M, Testarelli L, Gambarini G. A review of cyclic fatigue testing of nickel-titanium rotary instruments. *J Endod* 2009;35(11):1469-76.

Pruett JP, Clement DJ, Carnes DL. Cyclic fatigue testing of nickel-titanium endodontic instruments. *J Endod* 1997;23(2):77-85.

Santos LDA, Bahia MGDA, de Las Casas EB, Buono VT. Comparison of the mechanical behavior between controlled memory and superelastic nickel-titanium files via finite element analysis. *J Endod* 2013;39(11):1444-7.

Sattapan B, Nervo GJ, Palamara JE, Messer HH. Defects in rotary nickel–titanium files after clinical use. *J Endod* 2000;26(3):161-5.

Sattapan B, Palamara JE, Messer HH. Torque during canal instrumentation using rotary nickel-titanium files. *J Endod* 2000;26(3):156-60.

Schilder, H. Filling Root Canals in Three Dimensions. *Dent Clin North Am* 1967;723-44.

Schneider SW. A comparison of canal preparations in straight and curved root canals. *Oral Surg Oral Med Oral Pathol* 1971;32(2):271-5.

Shen Y, Qian W, Abtin H, Gao Y, Haapasalo M. Fatigue testing of controlled memory wire nickel-titanium rotary instruments. *J Endod* 2011;37(7):997-1001.

Shen Y, Cheung GSP. Methods and models to study nickel-titanium instruments. *Endod Topics* 2013;29(1):18-41.

Shen Y, Riyahi AM, Campbell L, Zhou H, Du T, Wang Z, Qian W, Haapasalo M. Effect of a combination of torsional and cyclic fatigue preloading on the fracture behavior of K3 and K3XF instruments. *J Endod* 2015;41(4):526-30.

Siqueira JF, Lopes HP. *Treatment of endodontic infections*. London: Quintessence;2011.

Spili P, Parashos P, Messer HH. The impact of instrument fracture on outcome of endodontic treatment. *J Endod* 2005;31(12):845-50.

Thompson SA. An overview of nickel–titanium alloys used in dentistry. *Int Endod J* 2000;33(4):297-310.

Walia H, Brantley WA, Gerstein H. An initial investigation of the bending and torsional properties of Nitinol root canal files. *J Endod* 1988;14(7):346-51.

Weine FS, Kelly RF, Lio PJ. The effect of preparation procedures on original canal shape and on apical foramen shape. *J Endod* 1975;1(8):255-62.

Weine FS. *Endodontic therapy*. St. Louis: CV Mosby;1982.